NaOH solution. The polymeric micelle that consisted of aldehyde-terminated PEG-PLA was finally obtained through dialysis against water for 24 h, which enabled the removal of the salt.

Effect of Both the pH and the Concentration of the Both Polymeric Micelle and the PAA Solutions on the Hydrogel's Gelation Properties

The hydrogel properties (storage modulus (G') and loss modulus (G'')) and the gelation time was determined by using an RS1 rheometer (Thermo Electron, Germany) at a gap of 1.0 mm and a shear stress of 1.0 Pa with a frequency of 1 Hz. The solutions containing either a polymeric micelle (5–30% w/w, pH 3–7 that was adjusted by HCl/NaOH, 0.1 mL) or PAA (5–20% w/w, pH 3–11 that was adjusted by HCl/NaOH, 0.1 mL) were introduced to the sample plate (15 mm in diameter) of the rheometer at 37°C. A two-pronged needle that consisted of two syringes was used. This needle is commonly used for mixing the solutions of the commercially available tissue-adhesive BOLHEAL™ (Kaketsuken Co., Japan).

Evaluation of the Hydrogel's Hemostatic Ability in a Mouse Hemostasis Model

A mouse hemostasis model was used for evaluation of the hydrogel's hemostatic ability according to the method which was previously reported in detail.[22] Briefly, the evaluation was performed according to the following procedure. Prior to experiments, a mouse received an intraperitoneal injection of pentobarbital sodium (Nembutal™, Dainippon Pharmaceutical Co., Japan). The procedure consisted of the following steps: (step 1) a mouse was fixed on a cork board, and its abdomen was incised; (step 2) serous fluid was carefully removed because it affected the estimation of the weight gained by the filter paper, and parafilm and preweighted filter paper were placed beneath the liver (parafilm prevented the filter paper's absorption of gradually oozing serous fluid); (step 3) the cork board was tilted and maintained at an angle of about 45° so that the bleeding would more easily flow from the liver toward the filter paper; and (step 4) the bleeding lasted for 3 min. In this step, a hemostat was applied to the liver wound immediately after the liver was pricked with a needle. Also, control experiments were performed (wherein a hemostat was not applied after the liver was pricked with a needle). We blinded the hemostat operator so that he could not know whether or not a hemostat was applied in each run (a blind test). The sterile needle (18G, 38 mm, Terumo Corp., Japan) was used for the pricking of the liver. Another experiment was conducted, in which a hemostat was applied to the unpricked liver to measure the amount of the excess aqueous solution that the filter paper absorbed. This experiment was important because the excess solution oozed out from the hemostat hydrogel during its formation. If this excess solution was not carefully determined and subtracted from the total amount of weight gained in the filter paper, the measured blood would be unjustly higher than the actual amount of blood through bleeding. Both the amount of the blood loss and the aqueous solutions were

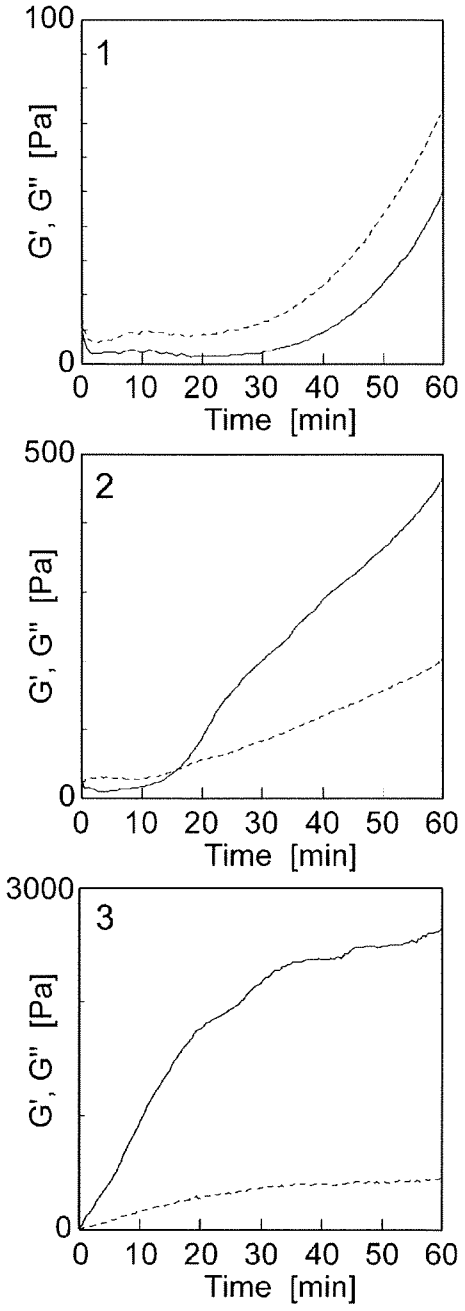

Figure 2. The storage modulus (G', solid line) and loss modulus (G'', dotted line) during the gelation when (1) the hydrogel was not formed, (2) the hydrogel was slowly formed, and (3) the hydrogel was rapidly formed. The pH of the polymeric micelle solution and the pH of the PAA solution are (1) 4 and 3, (2) 4 and 4, and (3) 4 and 9, respectively. The concentrations of the polymeric micelle solution and concentration of PAA solution are 30% w/w and 20% w/w, respectively.

TABLE I. Effect of Both the pH of the Polymeric Micelle Solution and the pH of the PAA Solutions on the Hydrogel's Gelation Properties[a,b,c]

The pH of the Polymeric Micelle Solution	The pH of the PAA Solution								
	3	4	5	6	7	8	9	10	11
3	21	75	759	1008	704	2013	3077	2199	1278
	(−)	(−)	(1847)	(321)	(49)	(1)	(1)	(1)	(1)
4	51	470	819	632	1714	2859	2640	1657	651
	(−)	(948)	(875)	(180)	(1)	(1)	(1)	(1)	(1)
5	98	753	405	1951	1462	1099	1208	975	479
	(2669)	(1203)	(468)	(440)	(1)	(1)	(1)	(1)	(1)
6	119	157	815	1102	1808	926	1432	488	171
	(3173)	(1923)	(354)	(1)	(1)	(1)	(1)	(1)	(1)
7	195	855	984	1790	1503	1269	1423	986	230
	(2409)	(1295)	(346)	(1)	(1)	(1)	(1)	(1)	(1)

[a] The values in the upper row show the storage modulus of the sample at 1 h (Pa), whereas those in the lower row (in parentheses) show the gelation time (s).
[b] −: Hydrogel was not formed.
[c] The concentrations of the polymeric micelle and PAA solutions were 30 and 20% w/w, respectively.

determined after removing the hydrogel from the filter paper. The case was excluded from the evaluation (~1/10 pricking procedures) when apparently projectile bleeding was induced (i.e., when the blood from the liver reached to the filter paper beneath the liver within 2 s after the withdrawal of the needle) owing to inappropriate operation such as ripping (not pricking) of the liver.

In this study, 16 ddY mice was used to evaluate the hemostatic potential of the hydrogel, and three ddY mice was used to estimate the amount of excess solution that oozed out during the hemostat formation. The average weight of the mice was 26.4 g (S.D. 1.7 g). All animal experiments were carried out according to the Principle of Laboratory Animal Care, the Guide for the Care and Use of Laboratory Animals, and guidelines of the animal care committee in our institute (Tokyo Women's Medical University). A statistical analysis of the data was performed by using the two-sided Student's t-test. A p value < 0.05 indicated statistical significance.

RESULTS

Evaluation of Factors Affecting the Hydrogel's Gelation Properties

Figure 2 shows the rheometer-determined gelation profile of the hydrogel. The gelation time is defined as the time when the solution phase changes from liquid-like behavior ($G' < G''$) to solid-like behavior ($G' > G''$).[23] As shown in Figure 2, three types of the gelation profiles were observed as follows: (1) the hydrogel was not formed (G' was lower than G''), (2) the hydrogel was formed slowly (G' became greater than G'' after more than 1 s), and (3) the hydrogel was formed rapidly (G' became greater than G'' within 1 s).

Table I summarizes the effects of the pH of both the polymeric micelle and the PAA solutions on hydrogel's storage modulus and gelation time. The storage modulus increased as the pH of the PAA solution increased from 3 to 8, when the pH of the polymeric micelle was 4. However, the storage modulus decreased as the pH of the PAA solution increased from 8 to 11. The gelation time was reduced within 1 s as the pH of either the polymeric micelle or the PAA solutions increased. These phenomena were observed in all cases when the pH of the polymeric micelle solution varied from 3 to 7. We achieved the fast gelation within 1 s in case when the pH of the PAA was over 6, 7, and 8 under the constant pH.

Table II summarizes the effects that concentrations of the polymeric micelle solution and of the PAA solutions have on the hydrogel's gelation properties. The storage modulus increased and the gelation time decreased as the concentrations of the polymeric micelle solution or of the PAA solution increased.

TABLE II. Effect of Both the Concentration of the Polymeric Micelle Solution and the Concentration of the PAA Solution on the Hydrogel's Gelation Properties[a,b]

The Concentration of the Polymeric Micelle Solution (w/w%)	The Concentration of the PAA Solution (w/w%)		
	5	10	20
5	143	167	223
	(845)	(351)	(118)
10	424	535	681
	(15)	(1)	(1)
20	1127	2168	2215
	(1)	(1)	(1)
30	1449	2788	3077
	(1)	(1)	(1)

[a] The values in the upper row show the storage modulus of the sample at 1 h (Pa), whereas those in the lower row (in parentheses) show the gelation time (s).
[b] The pH of the polymeric micelle and PAA solutions were 3 and 9, respectively.

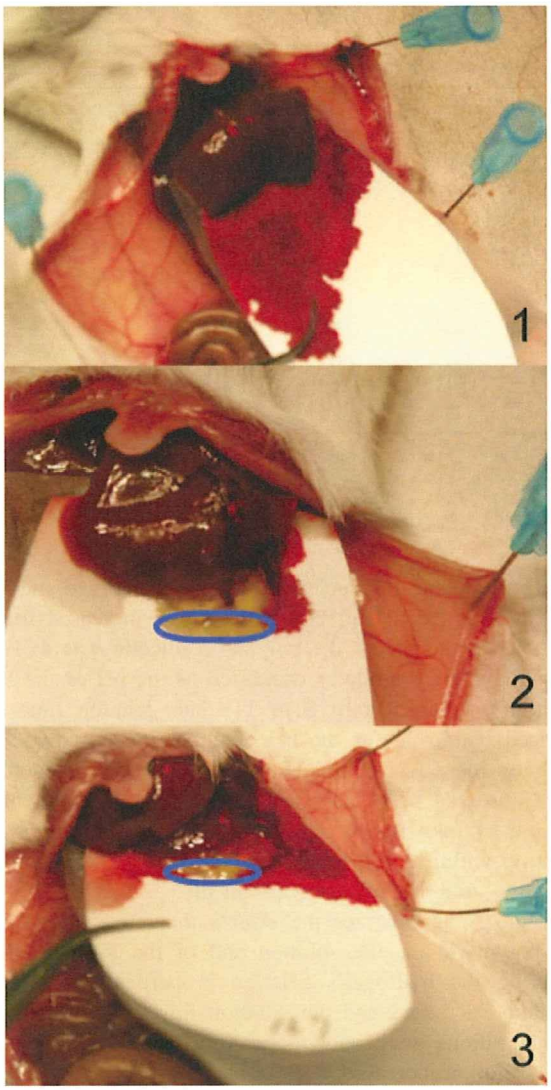

Figure 3. The evaluation of the hemostatic ability of the hydrogel (1: entry 12, 2: entry 1, and 3: entry 13). The blue circle shows the part of excess aqueous solution that oozed out from the hydrogel.

Evaluation of the Hemostatic Ability of the Hydrogel in a Mouse Hemostasis Model

Figure 3 shows typical photographs of hydrogel applications. Bleeding from the liver was allowed to continue during evaluation time (3 min after the liver was pricked with a needle) [Figure 3(1)]. On the other hand, the bleeding was completely arrested by the hydrogel application [Figure 3(2)]. In some cases of excessive bleeding, a part of the hydrogel moved slightly owing to a stream of the blood. Even in this case, the hydrogel inhibited bleeding considerably [Figure 3(3)].

Table III summarizes the results that concern the amount of bleeding with or without the hydrogel application. The average amount of the bleeding was 209.4 mg (s.d. 124.6 mg, $N = 8$) in the control experiments, whereas it was 86.5 mg (S.D. 24.0 mg, $N = 8$) when the hydrogel was applied to the wound ($p = 0.03$). Furthermore, the average amount of the excess solution was determined to be 59.3 mg (S.D. 5.7 mg, $N = 3$). By considering the amount of the excess solution, we could reevaluate the average amount of bleeding to be 27.2 mg (S.D. 24.0 mg, $N = 7$) when the hydrogel was applied to the wound ($p = 0.004$).

DISCUSSION

Evaluation of Factors Affecting the Hydrogel's Gelation Properties

Desired features of a tissue-adhesive local hemostat are high-gel strength and rapid gelation. The preliminary coagulometer-based evaluation[20] showed that the hydrogel was rapidly formed when the pH of the polyallylamine solution was higher than 7, whereas a white aggregate with a low storage modulus was formed when the PAA solution with a pH over 10 was used, in case the pH of the polymeric micelle solution was 5. For this article, a further accurate and quantitative evaluation was performed by using a rheometer that can quantitatively determine viscoelastic properties of materials.

Figure 2 shows the rheometer-determined gelation profile of the hydrogel. The rheometer gives the storage modulus (G') and loss modulus (G'') that characterize the elastic and viscous characteristics of a material, respectively. G' is nearly equal to the complex modulus (G^*) that reveals the degree of the elasticity of a material, and, G'' can be used

TABLE III. Evaluation of the Amount of Bleeding With (+) or Without (−) the Application of the Hydrogel

Entry	Hydrogel Application	Filter Paper[a] (mg)	Filter Paper + blood (mg)	Blood (mg)
1	+	149	227	78
2	−	150	436	286
3	+	148	214	66
4	+	125	189	64
5	−	156	367	211
6	+	173	275	102
7	−	134	201	67
8	+	155	228	73
9	−	150	251	101
10	+	184	262	78
11	−	189	414	225
12	−	192	365	173
13	+	167	303	136
14	−	201	348	147
15	+	192	287	95
16	−	182	323	465 (141 + 324)
		192	516	

[a] In entry 16, two filter papers were used.

as an indicator of gel strength.[23,24] Table I summarizes the effects of the pH of both the polymeric micelle and the PAA solutions on hydrogel's gelation properties. To avoid possible degradation of the PLA block in an alkaline solution, only the polymeric micelle solution at pH 7 or lower was used. The storage modulus and the gelation time greatly depended on the pH of the concentrations of both the polymeric micelle and the PAA solutions. For example, the storage modulus increased as the pH of the PAA solution increased from 3 to 8, when the pH of the polymeric micelle was 4. However, the storage modulus decreased as the pH of the PAA solution increased from 8 to 11. The gelation time was reduced within 1 s as the pH of either the polymeric micelle or the PAA solutions increased. These phenomena were observed in all cases when the pH of the polymeric micelle solution varied from 3 to 7. The pH wherein the hydrogel exhibited a maximal storage modulus shifted from 9 to 7 as the pH of the polymeric micelle solution increased from 3 to 7. We achieved the fast gelation within 1 s in case when the pH of the PAA was over 6, 7, and 8 under the constant pH (6 or 7, 4 or 5, and 3) of the polymeric micelle, respectively. The time required for hydrogel formation (1 s) was comparable to or shorter than that previously reported for other tissue-adhesive hydrogels.

The hydrogel was formed according to the Schiff base in a pH-dependent manner. Although the Schiff base formation reaction ($R_1—NH_2 + CHO—R_2 \rightleftharpoons R_1—N = CH—R_2 + H_2O$) proceeds faster at a slightly acidic pH,[25] the concentration of reactive R_1-NH_2 increases as pH increases because a primary amine obeys the equilibrium $R_1—NH_2 + H^+ \rightleftharpoons R_1—NH_3^+$. Thus, the hydrogel was rapidly formed as the pH of the PAA solutions increased. As the pH increased further, the enhanced Schiff base formation reaction made the PAA molecules cover the reactive surface of the polymeric micelle, decreasing the amount of the exposed aldehyde group on the micelle. Therefore, a white aggregate with low-storage modulus was formed as the pH of the PAA solution increased. The storage modulus greatly depended on the pH of both the polymeric micelle and the PAA solutions. The rheometer-determined gelation profile of the hydrogel agreed with the preliminary coagulometer-based gelation profile that was previously reported.[20] With the regard to the results, the optimal conditions for the formation of the hydrogel were the pH values of 3 for polymeric micelle solution and of 9 for the PAA solutions.

Concentrations of the solutions are another important factor affecting the hydrogel's properties (Table II). The storage modulus increased and the gelation time decreased as the concentrations of the polymeric micelle solution or of the PAA solution increased. The reason for these outcomes concerns the fact that the cross-linking density of the hydrogel increased as the concentration of gel-forming components increased. On the other hand, it was difficult to handle the polymeric micelle solution at a concentration of over 30% w/w and the PAA solution at a concentration of over 20% w/w owing to their overly hard viscosity. According to the results, the optimal condition for the formation of the hydrogel was that the concentrations of the polymeric micelle solution and of the PAA solution were 30% w/w and 20% w/w, respectively.

Evaluation of the Hemostatic Ability of the Hydrogel in a Mouse Hemostasis Model

The hemostatic ability of the hydrogel was evaluated in a mouse hemostasis model under the optimal conditions for the hydrogel formation obtained above (Figure 3, Table III). In one hydrogel-application case (entry 13), the hydrogel successfully arrested the bleeding even though projectile bleeding was observed. The average amount of the bleeding was 172.9 mg in the control experiments, whereas it was 79.4 mg when the hydrogel was applied to the wound ($p = 0.02$) without apparent outliers (entries 13 and 16) in which projectile bleeding was observed. The results indicated that the hydrogel possessed significant hemostatic potential and decreased a bleeding from a mice liver. Furthermore, it is noteworthy that the amount of excess solution that oozed out from the hydrogel [shown in Figure 3(2)] was not considered in the evaluation. Excess solution was oozed out from the hydrogel after the two precursor solutions were mixed. One will inaccurately determine the amount of bleeding to be excessively high if the effect of the amount of the excess aqueous solution is present in the determination: this caused the hemostatic ability of the hydrogel to be inaccurately estimated as low. By considering the amount of the excess solution, the average amount of bleeding was reevaluated to be 20.1 mg when the hydrogel was applied to the wound. These data demonstrated that the hydrogel had a highly significant hemostatic ability ($p = 0.002$). In another paper, we reported that a fibrin-based hemostat, Tisseel™ (Baxter, IL), had a relatively significant hemostatic potential ($p = 0.07$).[22] The difference between these two p values (0.002 and 0.07) shows that, compared with Tisseel, the hydrogel which was developed in this study possessed a significant hemostatic potential as a local hemostat.

CONCLUSIONS

In this study, a novel tissue-adhesive hydrogel containing a cross-linkable polymeric micelle consisting of PEG-PLA block polymers was examined. In particular, a rheometer was used to clarify the factors that affected the hydrogel's gelation properties. The storage modulus and the gelation time greatly depended on both the pH and the concentrations of both the polymeric micelle and the PAA solutions. Furthermore, we successfully demonstrated that the hydrogel both possessed a high-hemostatic ability and decreased bleeding from a mice liver.

Hydrogels have various functional properties, such as the ability to absorb a significant amount of water and flex-

ibility similar to a natural tissue. These properties have provided many potential applications particularly in biotechnological and medical fields.[26–29] The tissue-adhesive biomaterial, which was developed in this study, shows the novel medical application of hydrogels. Although several tissue-adhesive local hemostatic formulations have been developed for surgical applications to date, none of these are found to function in a completely satisfactory manner. The major drawbacks of these formulations include risk of infectious contaminations, high cytotoxicity, and complicated preparation methods. In contrast, our novel adhesive does not pose the risk of transmission of infectious contamination because the adhesive consists of only synthetic materials. The components of polymeric micelles (PEG and PLA) are known to be noncytotoxic and biocompatible. We used a macromolecular cross-linker that was expected to have low-tissue permeability, thereby reducing the risk of cytotoxicity. In addition, the hydrogel was easily obtained by mixing two precursor solutions. Therefore, although further optimization of a variety of factors (such as the structure of block polymers and polyamines) should be performed in the future for enhancement of the mechanical strength, the tissue-adhesiveness, and the biocompatibility of our hemostat, the results obtained in this study show that the hydrogel containing a cross-linkable polymeric micelle has the potential to address the need for a novel local hemostat.

REFERENCES

1. Tomizawa Y. Clinical benefits and risk analysis of topical hemostats: A review. J Artif Organs 2005;8:137–142.
2. Morikawa T. Tissue sealing. Am J Surg 2001;182:29S–35S.
3. MacGillivray TE. Fibrin sealants and glues. J Card Surg 2003;18:480–485.
4. Czerny M, Verrel F, Weber H, Muller N, Kircheis L, Lang W, Steckmeier B, Trubel W. Collagen patch coated with fibrin glue components. Treatment of suture hole bleedings in vascular reconstruction. J Cardiovasc Surg 2000;41:553–557.
5. Turner AS, Parker D, Egbert B, Maroney M, Armstrong R, Powers N. Evaluation of a novel hemostatic device in an ovine parenchymal organ bleeding model of normal and impaired hemostasis. J Biomed Mater Res 2002;63:37–47.
6. Taguchi T, Saito H, Uchida Y, Sakane M, Kobayashi H, Kataoka K, Tanaka J. Bonding of soft tissues using a novel tissue adhesive consisting of a citric acid derivative and collagen. Mater Sci Eng C 2004;24:775–780.
7. Fukunaga S, Karck M, Harringer W, Cremer J, Rhein C, Haverich A. The use of gelatin-resorcin-formalin glue in acute aortic dissection type A. Eur J Cardiothorac Surg 1999;15:564–570.
8. Kumar A, Maartens NF, Kaye AH. Evaluation of the use of BioGlue in neurosurgical procedures. J Clin Neurosci 2003;10:661–664.
9. Singer AJ, Thode HC. A review of the literature on octylcyanoacrylate tissue adhesive. Am J Surg 2004;187:238–248.
10. Ramakumar S, Roberts WW, Fugita OE, Colegrove P, Nicol TM, Jarrett TW, Kavoussi LR, Slepian MJ. Local hemostasis during laparoscopic partial nephrectomy using biodegradable hydrogels: Initial porcine results. J Endourol 2002;16:489–494.
11. Nakayama Y, Matsuda T. Photocurable surgical tissue adhesive glues composed of photoreactive gelatin and poly(ethylene glycol) diacrylate. J Biomed Mater Res 1999;48:511–521.
12. Ferland R, Mulani D, Campbell PK. Evaluation of a sprayable polyethylene glycol adhesion barrier in a porcine efficacy model. Hum Reprod 2001;16:2718–2723.
13. Wallace DG, Cruise GM, Rhee WM, Schroeder JA, Prior JJ, Ju J, Maroney M, Duronio J, Ngo MH, Estridge T, Coker GC. A tissue sealant based on reactive multifunctional polyethylene glycol. J Biomed Mater Res 2001;58:545–555.
14. Buchta C, Hedrich HC, Macher M, Hocker P, Redl H. Biochemical characterization of autologous fibrin sealants produced by CryoSeal and Vivostat in comparison to the homologous fibrin sealant product Tissucol/Tisseel. Biomaterials 2005;26:6233–6241.
15. Canonico S. The use of human fibrin glue in the surgical operations. Acta Biomed 2003;74:21–25.
16. Siedentop KH, Park JJ, Shah AN, Bhattacharyya TK, O'Grady KM. Safety and efficacy of currently available fibrin tissue adhesives. Am J Otolaryngol 2001;22:230–235.
17. Silver FH, Wang MC, Pins GD. Preparation and use of fibrin glue in surgery. Biomaterials 1995;16:891–903.
18. Ciapetti G, Stea S, Cenni E, Sudanese A, Marraro D, Toni A, Pizzoferrato A. Cytotoxicity testing of cyanoacrylates using direct contact assay on cell cultures. Biomaterials 1994;15:63–67.
19. Kaplan M, Baysal K. In vitro toxicity test of ethyl 2-cyanoacrylate, a tissue adhesive used in cardiovascular surgery, by fibroblast cell culture method. Heart Surg Forum 2005;8:E169–E172.
20. Murakami Y, Yokoyama M, Okano T, Nishida H, Tomizawa Y, Endo M, Kurosawa H. A novel synthetic tissue-adhesive hydrogel using a crosslinkable polymeric micelle. J Biomed Mater Res 2007;80A:421–427.
21. Nagasaki Y, Okada T, Scholz C, Iijima M, Kato M, Kataoka K. The reactive polymeric micelle based on an aldehyde-ended poly(ethylene glycol)/poly(lactide) block copolymer. Macromolecules 1998;31:1473–1479.
22. Murakami Y, Yokoyama M, Nishida H, Tomizawa Y, Endo M, Kurosawa H. A simple hemostasis model for the quantitative evaluation of hydrogel-based local hemostatic biomaterials on tissue surface. Colloids Surf B Biointerfaces 2008;65:186–189.
23. Ferry JD, Fitzgerald ER, Grandine LD, Williams ML. Temperature dependence of dynamic properties of elastomers: Relaxation distributions. Ind Eng Chem 1952;44:703–706.
24. Aklonis JJ, MacKnight WJ. Introduction to Polymer Viscoelasticity, 2nd ed. New York: Wiley; 1983.
25. Dohno C, Okamoto A, Saito I. Stable, specific, and reversible base pairing via Schiff base. J Am Chem Soc 2005;127:16681–16684.
26. Murakami Y, Maeda M. Hybrid hydrogels to which single-stranded (ss) DNA probe is incorporated can recognize specific ssDNA. Macromolecules 2005;38:1535–1537.
27. Murakami Y, Maeda M. DNA-responsive hydrogels that can shrink or swell. Biomacromolecules 2005;6:2927–2929.
28. van der Linden HJ, Herber S, Olthuis W, Bergveld P. Stimulus-sensitive hydrogels and their applications in chemical (micro)analysis. Analyst 2003;128:325–331.
29. Qui Y, Park K. Environmental-sensitive hydrogels for drugs delivery. Adv Drug Deliv Rev 2001;53:321–339.

Journal of Controlled Release 136 (2009) 240–246

Contents lists available at ScienceDirect

Journal of Controlled Release

journal homepage: www.elsevier.com/locate/jconrel

Histological study on side effects and tumor targeting of a block copolymer micelle on rats

Takanori Kawaguchi [a,b], Takashi Honda [b], Masamichi Nishihara [c], Tatsuhiro Yamamoto [c], Masayuki Yokoyama [c,*]

[a] Department of Pathology, Aizu Central Hospital, Aizu Wakamatsu 965-8611, Japan
[b] Division of Human Life Sciences, Fukushima Medical University School of Nursing, Hikariga-oka 1, Fukushima, Fukushima 960-1295, Japan
[c] Yokoyama Project, Kanagawa Academy of Science and Technology, KSP East 404, Sakado 3-2-1, Takatsu-ku, Kawasaki, Kanagawa 213-0012, Japan

ARTICLE INFO

Article history:
Received 11 September 2008
Accepted 12 February 2009
Available online 25 February 2009

Keywords:
Polymeric micelle
Pathology
Side effects
Block copolymer
Targeting

ABSTRACT

Histological examinations were performed with polymeric micelle-injected rats for evaluations of possible toxicities of polymeric micelle carriers. Weight of major organs as well as body weight of rats was measured after multiple intravenous injections of polymeric micelles forming from poly(ethylene glycol)-b-poly (aspartate) block copolymer. No pathological toxic side effects were observed at two different doses, followed only by activation of the mononuclear phagocyte system (MPS) in the spleen, liver, lung, bone marrow, and lymph node. This finding confirms the absence of – or the very low level of – in vivo toxicity of the polymeric micelle carriers that were reported in previous animal experiments and clinical results. Then, immunohistochemical analyses with a biotinylated polymeric micelle confirmed specific accumulation of the micelle in the MPS. The immunohistochemical analyses also revealed, first, very rapid and specific accumulation of the micelle in the vasculatures of tumor capsule of rat ascites hepatoma AH109A, and second, the micelle's scanty infiltration into tumor parenchyma. This finding suggests a unique tumor-accumulation mechanism that is very different from simple EPR effect-based tumor targeting.

1. Introduction

Recently, block copolymer micelles have gained considerable attentions as an efficacious carrier system of anti-cancer drugs [1–4]. Two objectives have been pursued with the polymeric micellecarriers; solubilization of water-insoluble drugs and targeting to solid tumors. Owing to a large loading capacity of the polymeric micelles' inner core for hydrophobic drugs, the polymeric micelles facilitate easy and safe intravenous injections of water-insoluble drugs such as paclitaxel [5,6]. The second objective, the targeting of the polymeric micelle carrier systems to solid tumors, is achieved by the targeting through the EPR (enhanced permeability and retention) effect [7,8]. For effective utilization of the EPR effect, poly(ethylene glycol) (PEG) has been used as an outer-shell-forming polymer block owing to its inert characteristics in interactions and uptake with or by bio-components such as proteins and cells. In particular, the PEG outer shell of the micelle is considered a critical factor in the reduction of micelle uptake by the mononuclear phagocyte system (MPS). For several anti-cancer drugs such as doxorubicin [2], cisplatin [9], and paclitaxel [10], the tumor targeting was successfully achieved in solid-tumor models in mouse. Research reported that, accompanying this targeting effect were diminished toxic side effects of the incorporated anti-cancer drugs: specifically, a reduction of nephrotoxicity [11] and pulmonary toxicity [12]. Furthermore, a paclitaxel-incorporating polymeric micelle enhanced the radiosensitizing activity of the drug [13]. Following these good results in animal evaluations, four clinical trials of polymeric micelle targeting are underway in 2008 for doxorubicin [14] paclitaxel [15], cisplatin [9], and SN-38 [16,17], the last of which is an active species of CPT-11.

The targeting efficiency and the toxic side effects of a given carrier are two important issues for drug targeting. In the "animal-tumor model" studies and the clinical-trial results mentioned above, carrier-based toxicities were not observed. In other words, the conclusion was that all the observed toxic side effects in animals and humans had resulted from either the anti-cancer drug delivered to normal organs and tissues or the drug released from the polymeric micelle carrier during its circulation in the bloodstream. Research has frequently noted the presence of carrier-based toxic side effects in drug targeting systems, and these side effects have included the hand–foot syndrome for a doxorubicin-incorporating liposome [18] and the infusion-related reactions for an antibody–anti-cancer drug conjugate [19]. These adverse effects can be a major concern in their clinical uses. Therefore, no or low toxicity in the polymeric micelle carriers seems a great advantage. Although the polymeric micelle systems are considered

* Corresponding author. Tel.: +81 44 819 2093; fax: +81 44 819 2095.
E-mail address: yp-yokoyama2093ryo@newkast.or.jp (M. Yokoyama).

0168-3659/$ – see front matter © 2009 Elsevier B.V. All rights reserved.
doi:10.1016/j.jconrel.2009.02.011

very safe carriers at least for anti-cancer drugs, it is worth while to conduct detailed histological and immunohistological examinations to identify the exact profiles and the exact mechanisms of the polymeric micelle carriers' possible toxic side effects. It is believed that these examinations can contribute not only to increasingly refined polymeric micelle designs for anti-cancer drug targeting, but also to polymeric micelles' applications to drugs other than anti-cancer drugs. In general, non-anti-cancer drugs exhibit milder toxic side effects than anti-cancer drugs. Even if carriers possess a low level of toxic side effects, these side effects may not be detected in the presence of strong toxic side effects of anti-cancer drugs. In such circumstance, it is not so important to examine the carriers' toxic effects in detail. In contrast, the carriers' toxic effects may be easily detected and be a problem in carriers' applications to non-anti-cancer-drugs that exhibit much milder side effects than anti-cancer drugs. Therefore, greater details in carriers' toxicity observation may be required for drug carriers' application to the non-anti-cancer drugs.

Concerning in vivo activities of polymeric micelles or of micelle-forming block copolymers, two interesting phenomena were reported: the depletion-of-ATP phenomenon and ABC (accelerated blood clearance) phenomenon. Kabanov et al. reported that Pluronic block polymers (poly(ethylene oxide)-b-poly(propylene oxide)-b-poly(ethylene oxide) block copolymers) could inhibit the activity of the protein playing a major role in multi-drug resistance through an ATP depletion mechanism [20,21]. The second ABC phenomenon is that clearance of long-circulating drug carriers is enhanced at the second dose through an immunological action. This phenomenon was reported by Dams et al. [22] and by Ishida et al. [23,24] for PEG-coated liposomes. Recently, this ABC phenomenon was also observed for a polymeric micelle carrier [25]. Therefore, it is challenging and interesting to examine detailed biological activities of PEG-based polymeric micelles whose distinctive activities or toxicities cannot be found in simple in vivo tests. No histological examinations, however, have been conducted for the polymeric micelle carriers that do not load any drug.

The current study analyzes acute biological activities of polymeric micelles forming from poly(ethylene glycol)-b-poly(aspartate) block copolymers that achieved successful tumor targeting of an anti-cancer agent camptothecin [26,27] and targeting of all-trans retinoic acid [28] by incorporation of these agents into the micelle. In this study, a term 'acute' is used to indicate a term of several weeks after the micelle injection. Therefore, the biological analysis is carried out for 30 days in the longest case. This study measured weight change of the whole body and major organs, and preformed histopathological observations with rats. Furthermore, a biotinylated polymeric micelle was prepared, and its tissue/cell distribution was analyzed with tumor-bearing rats. These evaluations and analyses provide valuable information on toxicity profiling of the polymeric micelle carriers, and may yield deep insight into polymeric micelles' targeting mechanism at solid-tumor sites.

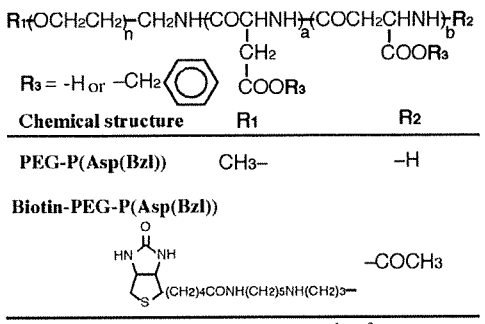

Chemical structure	R1	R2
PEG-P(Asp(Bzl))	CH_3–	–H
Biotin-PEG-P(Asp(Bzl))		–$COCH_3$

Composition	M.W. of PEG chain	number of Asp units (a + b)	benzyl ester content
PEG-P(Asp(Bzl))	5,200	24	89%
Biotin-PEG-P(Asp(Bzl))	4,900	25	82%

Fig. 1. Chemical structures and compositions of PEG-P(Asp(Bzl)) and biotin-PEG-P(Asp(Bzl)) block copolymers.

Table 1
Weights of major organs after polymeric micelle injections.

Dose	20 mg/kg×5[a]			200 mg/kg×5[b]		
	Polymeric micelle	Control[c]	Statistical significance[d]	Polymeric micelle	Control[c]	Statistical significance[d]
Brain	1.36±0.06	1.35±0.09	n.s.[e]	1.65±0.10	1.57±0.10	n.s.[e]
Heart	0.95±0.09	0.89±0.09	n.s.	0.58±0.06	0.67±0.07	n.s.
Lung	1.33±0.11	1.27±0.19	n.s.	1.21±0.08	1.44±0.12	n.s.
Liver	18.18±1.47	16.80±2.09	n.s.	10.60±1.08	10.55±0.67	n.s.
Spleen	0.70±0.09	0.64±0.10	n.s.	0.37±0.06	0.46±0.07	n.s.
Kidney	2.47±0.20	2.39±0.16	n.s.	1.61±0.16	1.73±0.16	n.s.

[a] Injections on days 0,1,3,5, and 7. Weights of organs were measured on day 30.
[b] Injections on days 0,1,2,3, and 4. Weights of organs were measured on day 7.
[c] Injections of physiological saline.
[d] By Student's *t*-test. Difference is considered significant when $p<0.05$.
[e] n.s.: not significant.

2. Materials and methods

2.1. Preparation of block copolymer micelle

Two block copolymers were synthesized. Their chemical structures are shown in Fig. 1. One block copolymer is poly(ethylene glycol)-block-poly(aspartate) (PEG-P(Asp(Bzl)), which possesses both a hydrophilic aspartic acid residue and a hydrophobic benzyl aspartate residue in one polymer block. This block copolymer was synthesized according to a previously reported method [29]. As summarized in Table 1, the PEG chain's average molecular weight of this block copolymer was 5200, and the average number of the Asp units was 24. The benzyl ester content was 89% with respect to the Asp unit. The other block copolymer is biotinyl-poly(ethylene glycol)-block-poly (benzyl aspartate) (biotin-PEG-P(Asp(Bzl)), which possesses almost the same composition as that of PEG-P(Asp(Bzl) except that the former features the terminal biotin moiety. In the current study, this biotinylated polymer was prepared according to the same method [29] with some modifications in the biotinylation at a polymer terminal. The starting material for this synthesis was α-amino propyl-ω-3,3-diethoxypropyloxy poly(ethylene glycol) (acetal-PEG-NH_2). The average molecular weight of this PEG block was 4900. Detailed synthetic procedures will be published elsewhere. In brief, the biotinylation was conducted according to a Schiff-base formation between the terminal aldehyde group and a biotinylation reagent, 5-(biotinamido)pentylamine (Pierce Biotechnology, Inc., Rockford, IL). The formed Schiff-base was reduced with sodium cyanoborohydride to obtain a stable secondary amine group as shown in Fig. 1. The obtained biotin-PEG-P(Asp(Bzl)) was characterized by means of ^{1}H NMR spectroscopy. From a ^{1}H NMR spectrum, conjugation of the biotin residue at the polymer terminal was found quantitatively (104%), and the benzyl ester content at the aspartic acid residue was determined to be 82%. The number of the aspartic acid residue was 25, and the molecular weight of this biotin-PEG-P(Asp(Bzl)) was 9700, as summarized in Fig. 1.

A polymeric micelle solution was prepared by means of a solvent-evaporation method as described previously [17]. The block copolymer was dissolved in chloroform. The solution was stirred in a glass bottle under a dry N_2 flow, allowing for evaporation of chloroform. Then, water was added to the dried residue, and sonication was applied so that a dispersed micelle solution would result. "Block copolymer micelle" solutions were stored at −30 °C until use. In non-biotinylated polymeric micelle preparations for toxicity evaluations, PEG-P(Asp(Bzl)) was used. In biotinylated micelle preparations, 10 mol% of biotin-PEG-P(Asp(Bzl)) and 90 mol% of (non-biotinylated)

PEG-P(Asp(Bzl)) (molecular weight of the PEG chain: 5200, number of Asp units: 24, benzyl ester content: 89%, and total molecular weight: 9800) were mixed and applied to the evaporation method.

2.2. Animal tests

2.2.1. Animals

Four-week-old to six-week-old female Donryu strain rats (60–80 g) were purchased from Chares River (Tokyo, Japan). The rats were maintained under water ad libitum and were used for experiments when they grew to 120–160 g. All animal experiments were carried out under the control of the Animal Research Committee in accordance with both the Guidelines on Animal Experiments in Fukushima Medical University, School of Medicine and the Japanese Government Animal Protection and Management Law.

2.2.2. Experimental design

Three types of experiments were carried out as stated below.

(1) Low-dose experiment
Rats received intravenous (i.v.) injections through a tail vein at a dose of 20 mg polymeric micelle/kg body weight in 0.5 ml physiological saline per day 5 times on days 0, 1, 3, 5, and 7. The micelle for the injection was formed from (non-biotinylated) PEG-P(Asp(Bzl)). The control rats received the same volume of physiological saline. Body weights of these rats were measured every other day until day 30. Six rats were used for the micelle-injected group, and six other rats were used for the control group. The rats were sacrificed on day 30 under deep ether anesthesia, and the weights of the brain, heart, lungs, liver, spleen, and kidneys were measured. The major organs and tissues (brain, thymus, lymph node, heart, lungs, liver, spleen, gastro-intestines, pancreas, kidneys, adrenal gland, ovary, uterus, muscle, and bone) were removed and were fixed in 10% formalin. These samples were processed for hematoxylin and eosin (HE) staining according to the standard method.

(2) High dose experiment
Rats received i.v. injections of a polymeric micelle at a dose of 200 mg polymeric micelle/kg body weight in 0.5 ml physiological saline per day 5 times at days 0, 1, 2, 3, and 4 and were sacrificed on day 8. The micelle for injection was formed with (non-biotinylated)PEG-P(Asp(Bzl)). The control rats received the same volume of physiological saline. The body weights of these rats were measured every day until day 7. Six rats were used for the micelle-injected group and the control group, each. Measurements of organ weights and their histological examinations were performed in the same manners as those for the low-dose experiment as described above.

(3) Histological observation with tumor-bearing rat
Rat ascites hepatoma AH109A cells [30], 4×10^6 cells/0.5 ml physiological saline, were inoculated, specifically in the subcutaneous tissues of the abdominal walls of 10 rats on day 0. Two rats received i.v. with 10 mg biotinylated micelles dispersed in 1 ml of physiological saline on day 2 and day 3 and were sacrificed 1 h and 1 day after the injection, respectively. This dose corresponds to approx. 60–80 mg/kg. On day 7, 6 rats received i.v. with 10 mg biotinylated micelles in 1 ml physiological saline. Two rats were sacrificed 1 h later, and other two rats were sacrificed 1 day later, and two other rats were sacrificed 1 week later. On day 14, two rats received i.v. with 10 mg biotinylated micelles. One rat was sacrificed 1 h later, and the other one was sacrificed 1 day later. All rats were sacrificed under deep ether anesthesia followed by Nembutal (pentobarbital sodium) anesthesia with circulation of physiological saline of 50–100 ml from the left ventricle to the right atrium.

2.3. Histology and immunohistochemistry

Histological materials were fixed in 10% formalin and embedded in paraffin, and then sections with 3 μm thickness were prepared. These thin sections were placed on glass slides, deparaffined in xylen, and dehydrated in graded alcohols. These slides were stained with hematoxylin and eosin (HE). Immunohistochemistry was performed according to a streptavidin–biotin complex method as described previously [31]. Briefly, endogenous peroxidase was blocked in 0.3% H_2O_2 in 100% methanol for 10 min. Some slides were sonicated for 10 min in a citrate buffer, pH 6.0. So that there would be a reduction in the nonspecific binding of the primary antibodies, sections were preincubated for 20 min at room temperature in 2% bovine serum albumin (BSA, Sigma, St. Louis, MO, USA). After washing with PBS, slides were covered with primary antibodies described below for overnight at 4 °C. Incubation with biotinylated secondary antibodies (Nichirei, Tokyo, Japan) was done at room temperature for 30 min. We applied a streptavidin–biotin–peroxidase complex (Nichirei, Tokyo, Japan or Vector Laboratories, Burlingame, CA, USA) to each slide. Binding was detected by hydrogen peroxidase/3,3′-diaminobenzidine tetrahydrochloride (DBA, Dojindo, Kumamoto, Japan). Hematoxylin was used for counterstaining. Sections with known expression of the respective epitope were used as positive controls, whereas the primary antibody was replaced with an antibody-dilution solution, serving as negative controls.

An anti-rat CD68 mouse monoclonal antibody was purchased from HyCult biotechnology b.v. (Uden, Netherlands). The antibody of 1 μg/100 μl PBS was applied to every slide. The mouse anti-biotin monoclonal antibody was purchased from Roche Diagnostic GmbH (Penzberg, Germany). The antibody of 1 μg/100 μl PBS was applied to every slide.

2.4. Statistical analysis

Data between groups were compared by means of Student's *t*-test. Differences were considered to be significant when $p<0.05$.

3. Results

3.1. Toxicity examinations

In the low-dose experiment (20 mg polymer/kg), the average body weight of the micelle-injected group was compared with that of the control group. As shown in Fig. 2, there was no statistically significant difference in body weights between the two groups although the micelle-injected group was slightly lighter than the control prior to the first injection. The weights of the brain, heart, lungs, liver, spleen, and kidneys of micelle-group rats did not differ from those of the control group as summarized in Table 1. No particular pathological

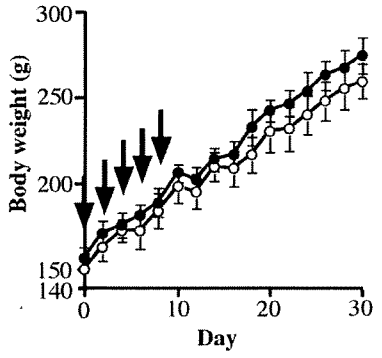

Fig. 2. Body-weight change in rats that received 20 mg/kg micelle or physiological saline 5 times (at arrows). No statistically significant differences were found between the micelle group and the control group.

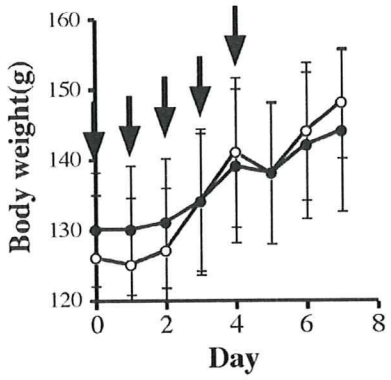

Fig. 3. Body-weight change in rats that received 200 mg/kg micelle or physiological saline 5 times at arrows. No statistically significant differences were found between the micelle group and the control groups.

changes were found in all these examined organs and tissues including bone marrow. Foamy cells were found focally in the lungs and lymph nodes in some rats as shown in Fig. 4a and c, respectively. Foamy-cell accumulation was observed in the lungs and the lymph nodes of the control group, but the degrees were milder than those of the micelle groups as shown in Fig. 4b and d.

Since no toxicity was observed in the low-dose experiment as stated above, a further pathological examination was carried out with an injected dose raised to 200 mg/kg so that there could be an accurate determination of any possible side effect of the micelle. The micelle was intravenously injected at 200 mg polymer/kg 5 times every day into rats, followed by (1) detailed examinations of body weight and organ weight, and (2) histology of organs/tissues. As shown in Fig. 3 and Table 1, there were no differences in the average body weight and in the average organ weight of rats between the micelle-treated group and the control group. In histological observations of HE sections, no abnormality was found in most examined organs and tissues.

One marked change in the micelle-treated group was seen: an increase of foamy cells in the spleen. This increase was observed in all treated rats as shown in Fig. 4e. This finding shows a clear contrast between the spleen of the micelle-injected group (Fig. 4e) and the spleen of the control (Fig. 4f). Staining with the anti-rat CD68 monoclonal antibody confirmed that the foamy cells were macrophages, as shown in Fig. 4g. Immunohistological examinations revealed marked increases in CD68-positive macrophages in the spleen, liver, lymph node, and lungs of the micelle-injected group when these sections were compared with those of the control group (Fig. 4g, i, and k for the rat injected with the micelle and Fig. 4h, j, and l for the control group.). The increase was much more dramatic in the spleen than in the liver and the lungs. The CD-68 immunohistological examination in lymph node was

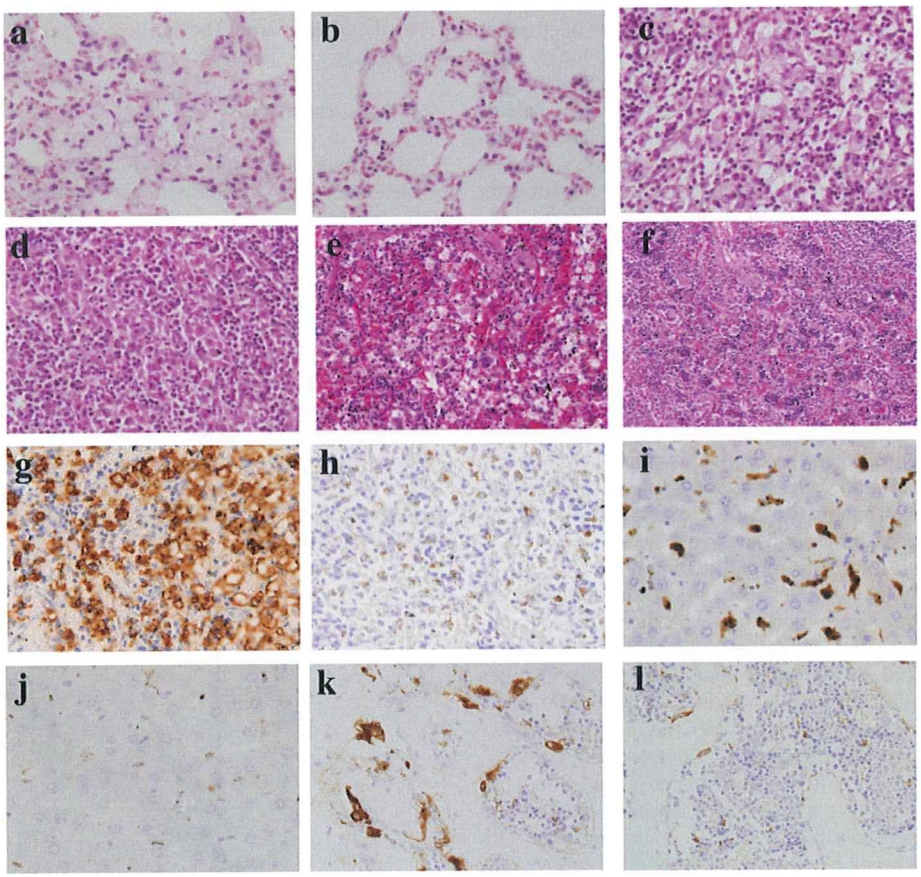

Fig. 4. Histological and immunohistochemical demonstrations of activated MPS in rats that received the micelle. ×400 in the original. (a)–(f): HE staining, and (g)–(l): immunostaining with mouse anti-rat CD68 monoclonal antibody. (a) and (c): accumulation of foamy cells in the lungs and lymph nodes, respectively, belonging to rats that received 20 mg/kg×5 times and were sacrificed at 30 days after the first injection of the micelle. (b) and (d): lungs and lymph nodes of the control groups, respectively. Foamy-cell accumulation was observed in the lungs and the lymph nodes of the control group, but the degrees were milder than those of the micelle groups. (e): foamy cells in the spleen. Foamy cells were accumulated in the spleens belonging to all rats that received 200 mg/kg×5 times and were killed at 7 days after the first injection of the micelle. (f): foamy-cell accumulation was rarely found in the spleen of control rats. Here is an immunohistochemical demonstration of activated MPS in (g) the spleen, (i) the liver, and (k) the lungs of the micelle-injected rats. Control mice exhibited smaller numbers of immunostaining-positive cells in (h) the spleen, (j) the liver, and (l) the lungs.

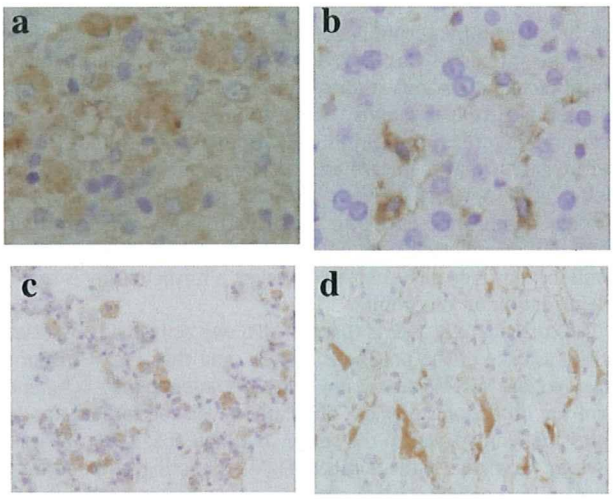

Fig. 5. Immunohistochemistry-based demonstration of biotinylated micelles. Anti-biotin antibody-positive signs were found on mononuclear cells in (a) the spleen, (b) the liver (Kupffer cells), and (c) the lungs (alveolar macrophage). Biotin-positive signs were also found in (d) renal tubules. These tissues were taken from a rat that bore a 2-week-old tumor and that had been sacrificed 24 h after the i.v. injection of 10 mg of biotinylated micelle / rat.

not done. From their intra-sinusoidal location and features, the foamy cells in the liver appeared to be Kupffer cells.

3.2. Microscopic observation of biotynylated micelle disposition with tumor-bearing rats

For immunohistological examinations, a biotinylated micelle was prepared (its chemical structure is shown in Fig. 1) for clarification of the micelle's accumulation behavior in tumor-bearing rats. One hour after the i.v. injection, no sign of the biotinylated micelle accumulation was found in most organs and tissues, including the spleen, liver, lungs, and lymph nodes. In contrast, biotinylated micelle-positive signs were found in the mononuclear phagocyte system (MPS) of the spleen, liver (Kupffer cells), and lungs 1 day after the injection, as shown in Fig. 5a–c. In addition, micelle accumulation was found in intra-tubules of kidneys (Fig. 5d). The biotinylated micelles were detected clearly in the MPS of the liver 1 week after the injection. (data not shown).

Disposition of the biotinylated micelle at the AH109A tumor was observed. As shown in Fig. 6a, the biotinylated micelle accumulation was evident as early as 1 h after injection in the blood vessels of the tumors that were transplanted 2 weeks before the micelle injection. This is a very interesting phenomenon because 1 h is a much shorter period than those are generally argued in targeting of the long-circulating drug carrier systems (e.g., PEG-coated liposomes and polymeric micelles) that utilize the EPR effect as a passive targeting strategy. It was reported that these long-circulating drug carrier systems provided the maximum delivery amounts at the tumor tissues 24 or 48 h post intravenous injection [18,33]. This unique and speedy micelle accumulation was also observed in younger 2-day-old and 1-week-old tumors. (The current study analyzed these tumors 2 days and 1 week after the tumor transplantation.) (data not shown) In enlarged images (Fig. 6b and c), most of the biotin-positive images were found in a highly concentrated manner. As shown in Fig. 6d, an elastic fiber staining image clearly indicates this is an arterial blood vessel.

This finding suggests that the observed micelles were aggregates of the micelles, not dispersed micelles. However, this issue needs further examination for confirmation of the observation in question.

The current study conducted this immunohistological examination both in the peripheral areas and the central areas of the tumor. Fig. 7a and b shows the immunohistological images of the peripheral and central parts, respectively. As shown in Fig. 7a for a 2 week-old tumor-bearing rat, the micelles were clearly observed in the blood vessels of tumor capsule 1 day after the micelle injection. The micelles were also observed in the tumor parenchyma (tumor cells, tumor interstitium of blood vessels, and fibrous tissue). The range of tumor parenchyma which showed the micelle-positive signs was approximate 200 μm, and the micelle-positive signs in the tumor parenchyma showed smaller and finer granular appearance than the micelle-positive signs in the capsular blood vessels. Fig. 7b shows that the micelles were also observed in the dilated and distorted blood vessels of the central tumor area, and that fine granular micelle-positive deposits were found in tumor cells neighboring to these blood vessels. This image was obtained 1 week after the i.v. injection of the micelle. These findings suggest that the observed micelles in the blood vessels were the aggregates of the micelles, while the micelles in the tumor parenchyma were the dispersed micelles. It is commonly accepted that delivery to a tumor's central area is very difficult owing to several inhibitory issues such as high interstitial pressure. In fact, the first paper concerning the EPR effect reported that macromolecules' delivery to the central area was much less effective than the delivery to the peripheral area [7]. Therefore, this micelle accumulation in the center area is interesting. The micelles were not clearly observed in extravascular space also in the case where the micelle accumulated in the central area of the tumor.

4. Discussion

The polymeric micelle drug carrier system is advantageous for a container of hydrophobic drugs owing to the hydrated micelle outer

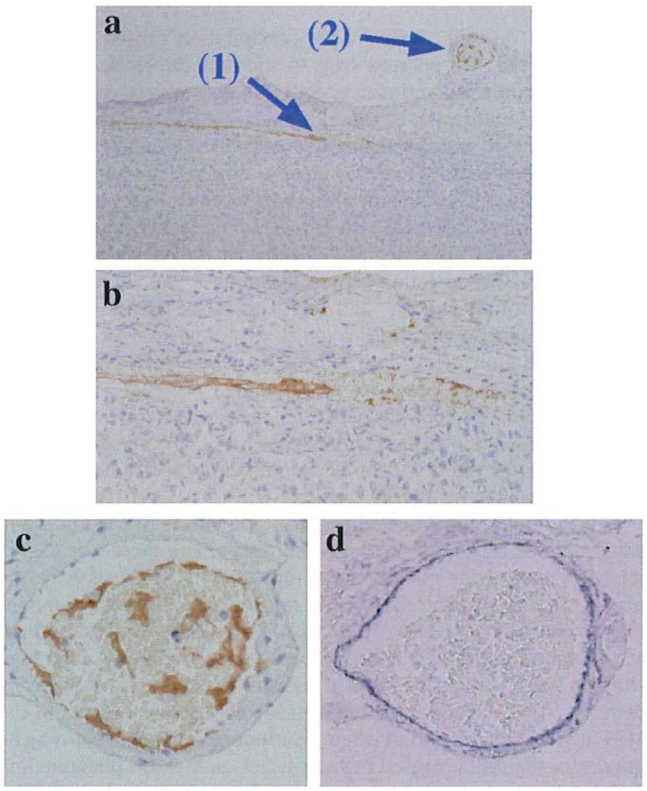

Fig. 6. Tumor targeting of biotinylated micelles. A rat with a 2-week-old tumor was injected with biotinylated micelles and was sacrificed under circulation of 100 ml physiological saline 1 h after the injection. (a) Blood vessels of peri-tumor connective tissues (capsule of tumor) exhibited strong anti-biotin antibody-positive signs. (b) Enlargement of arrow (1). The blood vessel seemed to be a capillary. (c) Enlargement of arrow (2). Anti-biotin antibody-positive signs were found along a blood-vessel surface in addition to a surface of a mass in the blood vessel. Some of the positive signs were seen in the blood. (d) Elastic fiber staining of panel c. This staining indicates that this is an arterial blood vessel.

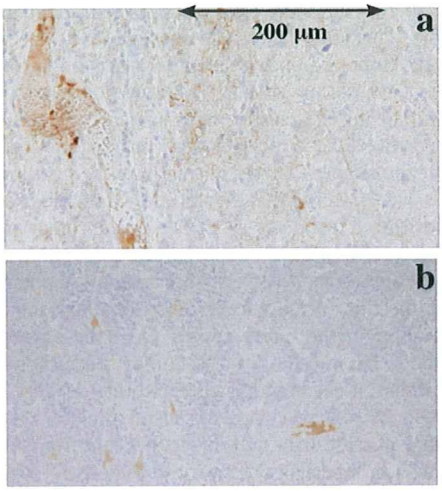

Fig. 7. Immunohistochemical observation of polymeric micelles at different areas of the tumor. (a) The micelles appeared in blood vessels of the tumor peripheral area. The material was taken from a 2-week-old-tumor 1 day after the i.v. injection of biotinylated micelle. The micelles appeared in the blood vessels of the tumor peripheral area (tumor capsule) and tumor parenchyma (tumor cells and tumor blood vessels) near the tumor capsule. (b) The micelles were detected in tumor blood vessels in the center area of the tumor 1 week after the i.v. injection into the 1-week-old-tumor. The micelles were detected in dilated and irregular-shaped blood vessels in center areas of the tumor 1 week after the i.v. injection into the 1-week-old tumor, where necrosis and degeneration occurred. The micelles were also detected in intact tumor cells around such blood vessels.

shell, which can effectively inhibit precipitation caused by hydrophobicity of the incorporated drug. In addition, the block copolymer micelle incorporating anti-cancer drug can accumulate selectively at tumor tissues by means of the EPR effect [7,8,32]. No studies have closely examined biological activities related to possible toxic side effects of the polymeric micelle carriers, although in vivo results for anti-cancer drug polymeric micelles suggested no or very low carrier-related toxicities. Concerning the EPR effect's selective accumulation, many reports have supported this EPR effect-based targeting strategy; nevertheless, several fundamental questions remain unelucidated: What parts of tumor tissues and vasculatures are the most active in exhibiting the EPR effect? How quick is permeation of polymeric micelles in tumor interstitium? And how dependent are the above-stated phenomena on the size of polymeric micelles? The authors have developed the PEG-P (Asp(Bzl)) micelle for anti-cancer drug targeting [26,27,29]. Using this PEG-P(Asp(Bzl)) micelle, the present study conducted the first detailed examinations of the acute in vivo effects of a polymeric micelle carrier.

The current study detected no toxic side effects of the micelle in any examined organs/tissues, even in cases where there was a large injection dose of the micelles (200 mg/kg×5). There was only one marked change in a micelle-treated rat: the activation of the mononuclear phagocyte system (MPS); also, the micelle exhibited a high accumulation in the MPS of the spleen, lungs, lymph node, and liver (Kupffer cells). This study constitutes the first report histologically demonstrating the accumulation of block copolymer micelles in the MPS in vivo. This activation is not a pathological change, but may be important to immunological reactions such as the ABC phenomenon [22–25]. Previous research reported that the polymeric micelle carrier system accumulated in the liver at a higher concentration than in other normal organs, and that the accumulated micelle remained present in the liver for a longer time than did a free drug [33]. One related point should be noted: it is evident that the biologically inert property of the PEG outer shell works efficiently to evade the MPS's very rapid micelle uptake, and, consequently, supports the micelle's long-circulation behavior in the bloodstream; however, this evasion was not perfect, providing a certain degree of the MPS uptake. In any case, because of this accumulation behavior of the micelle at the liver, strong liver toxicity was worrisome, but animal experiments and clinical results of various studies indicated that liver toxicities of the polymeric micelle systems were no more than those of the corresponding free drugs [9,14,15,33]. A possible reason for this mild liver toxicity is that the polymeric micelles accumulate only at liver's Kupffer cells, not at the liver's parenchymal cells (hepatocyte). As reported in our reference [9], the liver toxicities of doxorubicin-containing micelle evaluated with AST and ALT values were found to be milder than free doxorubicin. However, a further study is required for elucidation on this point.

The current study asserts that the MPS was activated in association with its uptake of the polymeric micelle, and that as a result of this activation, the MPS became foamy cells. In relation to the ABC phenomenon, an immunohistological observation was performed for IgM-expressing lymphocytes in the spleen at a high dose (200 mg/kg×5). However, no change in the number of IgM-expressing lymphocytes was observed in the spleen (data not shown). At present, the fate of the micelles that accumulated in the MPS cells has not been examined.

Interestingly, the current study found the biotinylated micelles in the blood vessels of tumors' peripheries (capsules) a very short time after the inoculation (1 h) and in the tumors' blood vessels 1 day after the injection. By using HPLC or radioisotope measurements of the accumulated amounts at tumor mass, preceding reports were able to show the tumor-selective accumulation of the polymeric micelles [2,10,16,27,34,35]. In these reports, the polymeric micelles showed the highest tumor accumulation at 24 h post intravenous injection. Thrombus seems at least in parts to be related to this micelle retention in the tumor blood vessels shown in Fig. 7. The EPR effect is known to facilitate the selective accumulation of the micelles at tumors. We observed much stronger micelle image in the blood vessel than in the tumor tissue 1 day after the injection with the immunostaning as shown in Fig. 7a. This observation suggests that the micelle-accumulation mechanism at specific sites of tumors is quicker than the accumulation driven by the EPR effect. However, only further studies can yield rigid evidence about the specific accumulation of micelles in the tumor blood vessels and the tumor tissues, because the research community generally believes that, when immunohistochemistry is the means, detection of dispersed micelles is more difficult to achieve than is detection of aggregates of micelles; and another general belief in the research community is that only dispersed micelles (not aggregated micelles) can be delivered by means of the EPR effect. (As described in the Results section, the micelles were found in tumor vasculatures in a highly concentrated manner, implying that the observed micelles were aggregates of the micelles rather than dispersed micelles.)

5. Conclusion

In this study's detailed histological examination, no pathological abnormality was observed for a systemic injection of PEG-P(Asp(Bzl)) polymeric micelles. The only marked change was activation of the MPS. These results confirmed the high safety of polymeric micelle drug carriers, but suggested the need of further investigation into polymeric micelles' interactions with the MPS. The immunohistochemical analyses also revealed very rapid and specific accumulation of the micelle in the vasculatures of tumor capsule of rat ascites hepatoma AH109A.

Acknowledgments

This work was supported by Grants-in-Aids from the Ministry of Health, Labour and Welfare of Japan. M. Nishihara, T. Yamamoto and M. Yokoyama acknowledge support from the Program for Promoting the Establishment of Strategic Research Centers, Special Coordination Funds for Promoting Science and Technology, and the Ministry of Education, Culture, Sports, Science, and Technology, Japan.

References

[1] M. Yokoyama, M. Miyauchi, N. Yamada, T. Okano, Y. Sakurai, K. Kataoka, S. Inoue, Characterization and anticancer activity of the micelle-forming polymeric anticancer drug adriamycin-conjugated poly(ethylene glycol)-poly(aspartic acid) block copolymer, Cancer Res. 50 (1990) 1693–1700.
[2] M. Yokoyama, T. Okano, Y. Sakurai, S. Fukushima, K. Okamoto, K. Kataoka, Selective delivery of adriamycin to a solid tumor using a polymeric micelle carrier system, J. Drug Target. 7 (1999) 171–186.
[3] R. Sevic, A. Eisenbberg, D. Maysinger, Block copolymer micelles as delivery vehicles of hydrophobic drugs: micelle–cell interactions, J. Drug Target. 14 (2006) 343–355.
[4] D. Sutton, N. Nasongkla, E. Blanco, J. Gao, Functionalized micelle systems for cancer targeted drug delivery, Pharm. Res. 24 (2007) 1029–1046.
[5] S.C. Kim, D.W. Kim, Y.H. Shim, J.S. Bang, H.S. Oh, S.W. Kim, M.H. Seo, In vivo evaluation of polymeric micellar paclitaxel formulation: toxicity and efficacy, J. Control. Release 72 (2001) 191–202.
[6] T.-Y. Kim, D.-W. Kim, J.Y. Chung, S.G. Shin, S.C. Kim, D.S. Heo, N.K. Kim, Y.-J. Bang, Phase I and pharmacokinetic study of Genexol-PM, a cremophor-free, polymeric micelle-formulated paclitaxel, in patients with advanced malignancies, Clin. Cancer Res. 10 (2004) 3708–3716.
[7] Y. Matsumura, H. Maeda, A new concept for macromolecular therapeutics in cancer chemotherapy: mechanism of tumoritropic accumulation of proteins and the antitumor agent smancs, Cancer Res. 46 (1986) 6387–6392.
[8] H. Maeda, L.W. Seymour, Y. Miyamoto, Conjugates of anticancer agents and polymers: advantages of macromolecular therapeutics in vivo, Bioconjug. Chem. 3 (1992) 351–361.
[9] H. Uchino, Y. Matsumura, T. Negishi, F. Koizumi, T. Hayashi, T. Honda, N. Nishiyama, K. Kataoka, S. Naito, T. Kakizoe, Cisplatin-incorporated polymeric micelle (NC-6004) can reduce nephrotoxicity and neurotoxity of cisplatin in rats, Br. J. Cancer 19 (2005) 678–687.
[10] T. Hamaguchi, Y. Matsumura, M. Suzuki, K. Shimizu, R. Goda, I. Nakamura, I. Nakatomi, M. Yokoyama, K. Kataoka, T. Kakizoe, NK105, a paclitaxel-incorporating micellar nanoparticle formulation, can extend in vivo antitumor activity and reduce the neurotoxicity of paclitaxel, Br. J. Cancer 92 (2005) 1240–1246.
[11] H. Uchino, Y. Matsumura, T. Negishi, F. Koizumi, T. Hayashi, T. Honda, N. Nishiyama, K. Kataoka, S. Naito, T. Kakizoe, Cisplatin-incorporated polymeric micelle (NC-6004) can reduce nephrotoxicity and neurotoxity of cisplatin in rats, Br. J. Cancer 19 (2005) 678–687.
[12] Y. Mizumura, Y. Matsumura, M. Yokoyama, T. Okano, T. Kawaguchi, F. Moriyasu, T. Kakizoe, Incorporation of the anticancer agent KRN5500 into polymeric micelles diminishes the pulmonary toxicity, Jpn. J. Cancer Res. 93 (2002) 1273-1243.
[13] T. Negishi, F. Koizumi, H. Uchino, J. Kuroda, T. Kawaguchi, S. Naito, Y. Matsumura, NK105, a paclitaxel-incorporating micellar nanoparticle, is a more potent radiosensitising agent compared to free paclitaxel, Br. J. Cancer 95 (2006) 601–606.
[14] Y. Matsumura, T. Hamaguchi, T. Ura, K. Muro, Y. Yamada, Y. Shimada, K. Shirao, T. Otsuka, H. Ueno, M. Ikeda, N. Watanabe, Phase I clinical trail and pharmacokinetic evaluation of NK911, a micelle-encapsulated doxorubicin, Br. J. Cancer 91 (2004) 1775–1781.
[15] T. Hamaguchi, K. Kato, H. Yasui, C. Morizane, M. Ikeda, H. Ueno, K. Muro, Y. Yamada, T. Okusaka, K. Shirao, Y. Shimada, H. Nakahama, Y. Matsumura, A phase I and pharmacokinetic study of NK105, a paclitaxel-incorporating micellar nanoparticle formulation, Br. J. Cancer 97 (2007) 170–176.
[16] F. Koizumi, M. Kitagawa, T. Negishi, T. Onda, S. Matsumoto, T. Hamaguchi, Y. Matsumura, Novel SN-38-incorporating polymeric micelles, NK012, eradicate vascular endothelial growth factor-secreting bulky tumors, Cancer Res. 66 (2006) 10048–10056.
[17] M. Sumitomo, F. Koizumi, T. Asano, A. Horiguchi, K. Ito, T. Asano, T. Kakizoe, M. Hayakawa, Y. Matsumura, Novel SN-38-incorporated polymeric micelle, NK012, strongly suppresses renal cancer progression, Cancer Res. 68 (2008) 1631–1635.
[18] D.C. Drummond, D. Kirpotin, C. Benz, J.W. Park, K. Hong, Liposomal drug delivery systems for cancer therapy, in: D.M. Brown (Ed.), Drug Delivery Systems in Cancer Therapy, Humana Press Inc., Totowa, 2004, pp. 191–213.
[19] P.R. Hamann, M.S. Berger, Mylotarg: the first antibody-targeted chemotherapy agent, in: M. Page (Ed.), Tumor Targeting in Cancer Therapy, Humana Press Inc., Totowa, 2002, pp. 239–254.
[20] A.V. Kabanov, J. Zhu, Luronic block copolymers for drug and gene delivery, in: G.S. Kwon (Ed.), Plymeric Drug Delivery Systems, Taylor & Francis, Boca Raton, 2005, pp. 577–613.
[21] E.V. Batrakova, S. Li, W.F. Elmquist, D.W. Miller, V.Y. Alakhov, A.V. Kabanov, Mechanism of sensitization of MDR cancer cells by Pluronic block copolymers: selective energy depletion, Br. J. Cancer 85 (2001) 1987–1997.
[22] E.T.M. Dams, P. Laverman, W.J.G. Oyen, G. Strom, G.L. Scherphof, J.W.M. van der Meer, F.H.M. Coretens, O.C. Boerman, Accelerated blood clearance and altered biodistribution of repeated injections of sterically stabilized liposomes, J. Pharmacol. Exp. Ther. 292 (2000) 1071–1079.
[23] T. Ishida, M. Ichihara, X. Wang, K. Yamamoto, J. Kimura, E. Majima, H. Kiwada, Injection of PEGylated liposomes in rats elicits PEG-specific IgM, which is responsible for rapid elimination of a second dose of PEGylated liposomes, J. Control Release 112 (2006) 15–25.
[24] T. Ishida, H. Kiwada, Accelerated blood clearance (ABC) phenomenon upon repeated injection of PEGylated liposomes, Int. J. Pharm. 345 (2008) 56–62.
[25] H. Koide, T. Asai, K. Hatanaka, T. Urakami, T. Ishii, E. Kenjo, M. Nishihara, M. Yokoyama, T. Ishida, H. Kiwada, N. Oku, The particle size-dependent occurrence of accelerated blood clearance phenomenon, Int. J. Pharm. 362 (2008) 197–200.
[26] M. Watanabe, K. Kawano, M. Yokoyama, P. Opanasopit, T. Okano, Y. Maitani, Preparation of camptothecin-loaded polymeric micelles and evaluation of their incorporation and circulation stability, Int. J. Pharm. 308 (2006) 183–189.
[27] K. Kawano, M. Watanabe, T. Yamamoto, M. Yokoyama, P. Opanasopit, T. Okano, Y. Maitani, Enhanced antitumor effect of camptothecin loaded in long-circulating polymeric micelles, J. Control Release 112 (2006) 329–332.
[28] N. Chansri, S. Kawakami, M. Yokoyama, T. Yamamoto, P. Charoensit, M. Hashida, Anti-tumor effect of all-*Trans* retinoic acid loaded polymeric micelles in solid tumor bearing mice, Pharm. Res. 25 (2008) 428–434.
[29] M. Yokoyama, P. Opanasopit, Y. Maitani, K. Kawano, T. Okano, Polymer design and incorporation method for polymeric micelle carrier system containing water-insoluble anti-cancer agent camptothecin, J. Drug Target. 12 (2004) 373–384.
[30] T. Kawaguchi, S. Imai, S. Haga, J. Morimoto, T. Honda, in: K. Watanabe (Ed.), Cancer Metastases Research, Nova Science Publisher, 2008, pp. 147–163.
[31] S.M. Hue, L. Raine, H. Fanger, Use of avidin–biotin–peroxidase complex (ABC) in immunoperoxidase techniques: a comparison between ABC and unlabeled antibody (PAP) procedures, J. Histochem. Cytochem. 29 (1981) 577–580.
[32] F.M. Muggia, Doxorubicin-polymer conjugates: further demonstration of the concept of enhanced permeability and retention, Clin. Cancer Res. 5 (1999) 7–8.
[33] M. Yokoyama, T. Okano, Y. Sakurai, H. Ekimoto, C. Shibazaki, K. Kataoka, Toxicity and antitumor activity against solid tumors of micelle-forming polymeric anticancer drug and its extremely long circulation in blood, Cancer Res. 51 (1991) 3229–3236.
[34] G.S. Kwon, S. Suwa, M. Yokoyama, T. Okano, Y. Sakurai, K. Kataoka, Enhanced tumor accumulation and prolonged circulation times of micelle-forming poly(ethylene oxide–aspartate) block copolymer–adriamycin conjugates, J. Control Release 29 (1994) 17–23.
[35] N. Nishiyama, S. Okazaki, H. Cabral, M. Miyamoto, Y. Kato, Y. Sugiyama, K. Nishio, Y. Matsumura, K. Kataoka, Novel cisplatin-incorporated polymeric micelles can eradicate solid tumors in mice, Cancer Res. 63 (2003) 8977–8983.

Journal of Controlled Release 136 (2009) 187–195

Contents lists available at ScienceDirect

Journal of Controlled Release

journal homepage: www.elsevier.com/locate/jconrel

Encapsulation of the synthetic retinoids Am80 and LE540 into polymeric micelles and the retinoids' release control

Taku Satoh [a], Yuriko Higuchi [b], Shigeru Kawakami [b], Mitsuru Hashida [b], Hiroyuki Kagechika [c], Koichi Shudo [d], Masayuki Yokoyama [a,*]

[a] Yokoyama Project, Kanagawa Academy of Science and Technology, KSP East 404, Sakado 3-2-1, Takatsu-ku, Kawasaki, Kanagawa 213-0012, Japan
[b] Department of Drug Delivery Research, Graduate School of Pharmaceutical Sciences, Kyoto University, Sakyo-ku, Kyoto 606-8501, Japan
[c] School of Biomedical Science, Tokyo Medical and Dental University, Kanda-surugadai 2-3-10, Chiyoda-ku, Tokyo 101-0062, Japan
[d] Research Foundation Itsuu Laboratory, Tamagawa 2-28-10, Setagaya-ku, Tokyo 158-0094, Japan

ARTICLE INFO

Article history:
Received 25 December 2008
Accepted 27 February 2009
Available online 14 March 2009

Keywords:
Polymeric micelle
Retinoid
Ion-pairing
Sustained release
Controlled release

ABSTRACT

The objective of this study was to encapsulate two synthetic retinoids Am80 and LE540 into polymeric micelles and to control the retinoids' release rate in vitro. Highly efficient encapsulation yields of these retinoids were obtained for micelles forming from PEG-poly(benzyl aspartate) block copolymers in the wide range of the benzyl substitution degree. The in vitro release examination for LE540 indicated very stable encapsulation of this retinoid owing to its strongly hydrophobic nature. On the other hand, Am80 exhibited a rapid release in Dulbecco's phosphate buffer saline. An addition of a hydrophobic alkyl amine in the Am80-encapsulation process successfully led to significant retardation of the Am80 release rate. A mechanism of the retardation was considered an increase of Am80 hydrophobicity due to an ion-pairing with the alkyl amine. This paper is the first report on release control in the polymeric micelle carrier system through the ion-pairing between an encapsulated drug and an additive.

1. Introduction

Polymeric micelles are self-assembling nanostructures that are typically composed of amphiphilic block copolymers [1]. Micelles have recently received much attention as a promising drug delivery carrier because a large quantity of hydrophobic drugs can be encapsulated into the micelle core in a stable manner. In systemic administration the drug-encapsulating micelles are expected to demonstrate various advantages; e.g., long-circulation in the blood stream owing to the nano-size and the hydrated-surface property of the micelles, and selective accumulation at tumor tissues owing to the EPR effect [2].

For drug targeting with the polymeric micelle carriers, research and development have focused on hydrophobic and cytotoxic anti-cancer drugs such as doxorubicin [3], paclitaxel [4], and camptothecin and its analogues [5,6]. These drugs cause cell mortality by means of strong cellular dysfunction. We would like to explore an application of polymeric micelle delivery using another type of drug that expresses pharmacological activities by regulating cellular functions. We have selected retinoids for this purpose [7,8].

Retinoids were originally defined as vitamin A and its analogues [9]. Compounds in this family modulate specific nuclear receptors called retinoic acid and retinoid X receptors (RARs and RXRs). Each of these receptors includes three subtypes (α, β, and γ). By binding to these receptors retinoids regulate cellular events including differentiation, proliferation, and apoptosis [10,11]. All-trans retinoic acid (ATRA) is clinically approved against acute promyelocytic leukemia (APL). This is the first approval of the differentiation therapy against cancer, indicating retinoids' high potency in clinical applications [12]. In an updated definition, retinoids are expanded to include molecules that bind to RARs and RXRs [13,14], regardless of their similarity in molecular structure to vitamin A. Researchers have reported that synthetic retinoids, such as 6-[3-(1-adamantyl)-4-hydroxyphenyl]-2-naphthalene carboxylic acid (CD437) [15] and *N*-(4-hydroxyphenyl) retinamide (4-HPR) [16], have induced apoptosis in neoplasma. Although researchers have not yet fully elucidated the mechanism underlying the related actions of these synthetic retinoids, CD437- and 4-HPR-induced apoptosis includes an RAR-independent pathway. Many other synthetic retinoids have been designed to improve pharmacological effects and to decrease adverse effects [17,18].

For the current research project, we selected two synthetic retinoids, Am80 and LE540, as encapsulated drugs (Chart 1). One reason for our decision to select these retinoids is their attractive pharmacological activities. Am80, an RAR-α/β specific agonist, was approved in Japan in 2005 for relapsed or refractory APL [19]. Its antimyeloma [20] and atherosclerosis inhibition effects in vivo have also been reported [21]. Since this synthetic retinoid has little binding affinity to cellular retinoic acid-binding proteins (CRABP),

* Corresponding author. Present address: Medical Engineering Laboratory, Research Center for Medical Science, Jikei University School of Medicine, 3-25-8, Nishi-Shimbashi, Minato-ku, Tokyo 105-8461, Japan. Tel.: +81 3 3433 1111x2336; fax: +81 3 3459 6005.
E-mail address: masajun2093ryo@jikei.ac.jp (M. Yokoyama).

0168-3659/$ – see front matter © 2009 Elsevier B.V. All rights reserved.
doi:10.1016/j.jconrel.2009.02.024

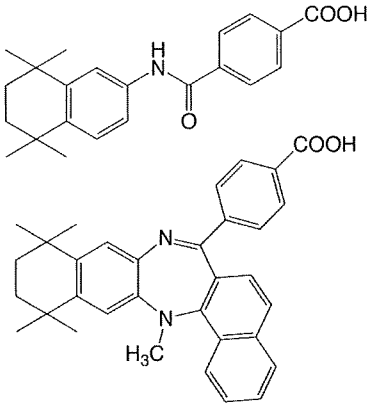

Chart 1. Am80 and LE540 (top and bottom).

CRABP-dependent retinoid-resistance will be avoided. Moreover, Am80 is much more stable than ATRA in the contexts of light, heat, and oxidation. In comparison, LE540 is an RAR antagonist, and its inhibition activity for Am80-induced HL-60 cell differentiation has been reported [22]. Targeting and the controlled release of these retinoids through micelle encapsulation will expand their therapeutic applications, especially when the target is solid tumor tissue for Am80.

Chemical-structure characteristics of Am80 and LE540 constitute the other reason for the selection. We use the hydrophobic frames of these retinoids to encapsulate the compounds into micelles. As compared with Am80, LE540 has bulkier hydrophobic moiety. Therefore, these two retinoids not only possess high therapeutic potential, but also benefit analysis on relations between the chemical structures of drugs and the corresponding encapsulation-release behaviors of the retinoids.

In this study, we perform encapsulation of Am80 and LE540 into micelles forming from PEG-poly(benzyl aspartate) block copolymers and analyze the retinoids' encapsulation behaviors and release rates. Am80 and LE540 are sufficiently hydrophobic in water for easy and efficient encapsulation into a polymeric micelle. However, Am80 is soluble in Dulbecco's phosphate buffered saline (D-PBS) and is rapidly released from a polymeric micelle. Therefore we have attempted to control the release rates by means of an addition of hydrophobic compounds interacting with Am80. This is a novel methodology for the control of drug-release rates from polymeric micelle carriers. Even though addition of oppositely charged hydrophobic compounds have been frequently used in traditional drug carriers such as microparticles, the first time application of this method for the polymeric micelle carriers is very important. The reason for the importance is that extremely stable drug encapsulation (e.g., 10^{-19} cm^2/s diffusion coefficient [23]) is required due to a very small micellar inner core such as 10 nm in diameter as a drug container.

2. Materials and methods

2.1. Materials and equipment

For the present study, α-methoxy-ω-amino poly(ethylene glycol) (MeO-PEG-NH_2) (Mw 5-kDa) was purchased from NOF Corp. (Tokyo, Japan). And β-benzyl L-aspartate was purchased from Kokusan Chemical (Tokyo, Japan). Triphosgene was obtained from Tokyo Chemical Industry Co., Ltd. (Tokyo, Japan) and used as received. β-Benzyl L-aspartate *N*-carboxyanhydride (BLA-NCA) was prepared from β-benzyl L-aspartate and triphosgene according to the conventional method [24]. DMF was distilled at a reduced pressure before use. All other reagents used were of reagent grade. ^{1}H-NMR measurements were carried out with a Varian Unity Inova NMR spectrometer (Varian Technologies Japan Ltd., Tokyo, Japan) at 400 MHz. A Spectra/Por 6 dialysis membrane (Spectrum Laboratories Inc., CA, USA) (1-kDa cut-off) was used for dialysis. An HPLC analysis was carried out with an HPLC system (PU-2080 plus pump; MX-2080-32 dynamic mixer; UV-2070 plus UV detector; and RI-2031 plus RI detector, Jasco Corp., Tokyo, Japan) equipped with a TSK-gel ODS-80Ts reverse-phased column (150 × 4.6 mm i.d., Tosoh Corp., Tokyo, Japan). Dynamic light scattering (DLS) measurements were performed in 1.0% (w/w) aqueous solutions at 25 °C with a DLS-7000 (Otsuka Electronic Co. Ltd., Osaka, Japan). Particle size distribution in terms of weight fractions was calculated using a non-negative least squares (NNLS) algorithm.

2.2. Synthesis of amphiphilic diblock copolymers

Polymers used for encapsulation of retinoids are composed of a PEG-poly(aspartic acid) (PEG-P(Asp)) main chain and pendant benzyl groups (Table 1). PEG-poly(benzyl L-aspartate) (PEG-PBLA) polymers **1** and **2** were prepared by ring-opening polymerization of BLA-NCA from a primary amino terminal of MeO-PEG-NH_2 [25]. The PEG-P(Asp(Bzl)$_x$) polymers **3**–**5** were obtained as follows: (1) complete removal of benzyl groups from PEG-PBLA [26], and (2) partial esterification of PEG-P(Asp) with benzyl bromide (BzlBr) [27].

2.2.1. Synthesis of PEG-b-poly(β-benzyl L-aspartate) (PEG-PBLA)

PEG-b-poly(β-benzyl L-aspartate) (PEG-PBLA) block copolymers were synthesized according to literature [25]. Amino-terminated poly (ethylene glycol) MeO-PEG-NH_2 as a macroinitiator was mixed with BLA-NCA in a dichloromethane–DMF mixed solvent (9:1 v/v), and this mixture was stirred at 35 °C for 17 h under a nitrogen atmosphere. The reaction mixture was dropwisely added into diethyl ether cooled in ice. The resulting precipitate was collected by filtration, washed with diethyl ether, and dried under a reduced pressure. The degree of polymerization (DP, i.e., the average unit number of polymer chain) of the PBLA block was determined by ^{1}H-NMR spectroscopy in chloroform-*d*. The determination was based on an integration ratio between the proton assigned to the methylene of PEG (3.8–3.4 ppm) and the benzyl methylene of PBLA (5.2–4.9 ppm). The polymers **1** and **2** were estimated to be 24 and 28, respectively.

Table 1
Synthesis of PEG-P(Asp (Bzl)$_x$) block copolymers.

Polymer	Source						Product	
	PEG-P(Asp)[a]	BzlBr		DBU		BnBr/DBU	Yield	D.s. Bzl[b]
	g (Asp mmol)	g (mmol)	mol.eq./Asp	g (mmol)	mol.eq./Asp		(mg)	(%)
3	0.501 (1.51)	0.261 (1.52)	1.01	0.200 (1.31)	0.87	1.16	0.597	80
4	0.501 (1.51)	0.172 (1.00)	0.66	0.141 (0.93)	0.61	1.08	0.531	53
5	0.501 (1.51)	0.115 (0.67)	0.44	0.093 (0.61)	0.40	1.10	0.516	33

[a] PEG-P(Asp) 5-24 was prepared by hydrolysis of PEG-PBLA 2.
[b] Degree of benzyl substitution.

2.2.2. Synthesis of PEG-b-poly(aspartic acid) (PEG-P(Asp))

Benzyl ester of PEG-PBLA **2** was hydrolyzed in 0.5 M aqueous sodium hydroxide solution (3 mol.eq. to benzyl group) at r.t. In approximately 20 min, a suspension of the polymer changed into a transparent solution owing to hydrolysis. The resulting solution was acidified with 6 M hydrochloric acid, dialyzed against water, and freeze-dried. Chemical structures of products were analyzed by ^{1}H-NMR spectroscopy in deuterium oxide containing sodium deuteroxide. The peaks assigned to the benzyl group completely disappeared on the spectrum, indicating hydrolysis of the benzyl ester. The DP of the poly(aspartic acid) chain decreased from 28 to 24 in this step. It was also confirmed that the α-amide bond in the PBLA main chain was converted into the mixture of α- and β-amides (ca. 1:3) as described in previous reports [26,28].

2.2.3. Synthesis of partially benzyl-substituted PEG-P(Asp) (PEG-P(Asp (Bzl)x))

Partially benzyl-substituted PEG-P(Asp) (PEG-P(Asp $(Bzl)_x$)) polymers **3–5** were obtained by esterification of PEG-P(Asp) with benzyl bromide in the presence of 1,8-diazabicyclo[5.4.0]undec-7-ene (DBU) as reported in a previous paper [29]. The number *x* in the PEG-P(Asp $(Bzl)_x$) formula represents a percentage (%) of benzyl ester in the aspartic acid residues. PEG-P(Asp) was dissolved to DMF and was added by means of BzlBr and DBU, and the reaction mixture was stirred at 50 °C for 16 h under a nitrogen atmosphere. Polymers **3**, **4**, and **5** were obtained when BzlBr was added in 1.01, 0.66, and 0.44 mol. eq. to the aspartic acid unit, respectively, while the BzlBr/DBU mole ratio was almost constant ca. 1.1. The reaction mixture was dropwisely added into diethyl ether. The resulting precipitate was collected by filtration, washed with diethyl ether, and dried under a reduced pressure. For removal of DBU, the polymers were dissolved into DMF, followed by the addition of 6 M hydrochloric acid (1 mol.eq. to DBU), and then this mixture solution was dialyzed against water. The purified products were freeze-dried and analyzed by ^{1}H-NMR spectroscopy in DMSO-d_6 containing 3% trifluoroacetic acid. Table 1 summarizes the degree of benzyl substitution determined from a proton integration ratio between methylene of PEG (3.7–3.4 ppm) and methylene of the benzyl group (5.1–5.0 ppm).

2.3. Preparation of micelles

Drug-encapsulating micelles were obtained by a solvent evaporation method [30]. The process was as follows: the block copolymer (20 mg) and the drug (2.0 mg) were dissolved in THF (2.5 mL). Evaporation of THF with stirring at 40 °C under a dry nitrogen-gas flow provided a residue of the polymer and the drug as a thin-film. The residue was further dried under a reduced pressure, and then added by water (4.0 mL). A drug-encapsulating micelle was formed by subsequent sonication with a VCX-750 sonicator equipped with a 5 mm diameter microtip (Sonic & Materials Inc., CT, USA). The sonication was operated at 21% amplitude with 80-cycle of a 0.5 s pulse followed by a 1.0 s pause, at r.t. The micelle solution was centrifuged to remove a possible insoluble precipitate (3900 rpm, 10 min, 20 °C) and then filtered through a Millex 0.22 μm PVDF filter (Nihon Millipore K.K., Tokyo, Japan). The obtained micelle solution was stored at −30 °C before use. Empty micelles were prepared according to the same procedure in the absence of drug. When an additive compound was used, the compound was mixed in the initial polymer-drug solution.

2.4. Measurements of drugs encapsulated in micelles

Drug amounts recovered in the micelle solutions were determined by reversed phase HPLC. The mobile phase involved methanol–5% acetic acid aqueous solution mixture at 2:1 (v/v) for Am80 and 9:1 (v/v) for LE540. A flow rate was 1.0 mL/min at 40 °C. Detection was carried out by absorption at 290 nm and 356 nm for Am80 and LE540, respectively.

2.5. In vitro drug release

The drug-encapsulating micelle solution (1.0 mL) was filled in a dialysis tube and dialyzed against 100-fold volume of water or Dulbecco's phosphate buffer saline (D-PBS, pH 7.4) with stirring at r.t. An aliquot of the dialysate was freeze-dried prior to the addition of methanol (100 μL). After centrifugation (10,000 g, 10 min, r.t.), the resulting supernatant was applied to the reverse-phased HPLC system for measurements of the released drugs. This drug-release assay was performed in triplicate except as described elsewhere. The error bars represent the standard deviation.

2.6. Measurements of N,N-dimethyldodecylamine (DMDA) encapsulated in micelles

The micelles of polymer **1** (20 mg) were prepared through the evaporation–sonication process in the presence of Am80 (2.0 mg, 5.69 μmol) and *N,N*-dimethyldodecylamine (DMDA, 1.2 mg, 5.69 μmol) in water (4.0 mL). After the centrifugation and filtration, the resulting solution (500 μL) was ultrafiltered (10,000 *g*, 25 min, r.t.) with a Microcon YM-100 centrifugal filter unit (Nihon Millipore K.K., Tokyo, Japan). Fresh water (200 μL) was added to a retentate and ultrafiltered again (10,000 *g*, 20 min, r.t.). This water-addition–ultrafiltration cycle was repeated three times. The retentate and the filtrate were collected and their contents of Am80 and DMDA were determined by means of a reversed-phase HPLC. Measurement conditions for DMDA were as follows: the mobile phase was methanol–water at 9:1 (v/v) containing 0.1% (v/v) of triethylamine, the flow rate was 1.0 mL/min at 40 °C, and detection of DMDA was carried out with an RI detector. This experiment was performed in triplicate. The other sample solutions containing different compositions were prepared for the comparison as shown in Table 5.

2.7. Statistics

Each release study was performed in triplicate except for specifically indicated cases. Data were expressed as the mean ± standard deviation (SD). Statistical comparisons were performed by the use of two-tailed Student's *t*-test for two-groups, and Dunnett's method by the use of a JMP Version 6 Japanese edition software (SAS Institute Japan, Tokyo) for multiple groups.

3. Results and discussion

3.1. Preparation of drug-encapsulating micelles

PEG-PBLA polymers **1** and **2** were successfully prepared according to literatures (see experimental section). Polymer **2** was converted into PEG-P(Asp $(Bzl)_x$) **3–5** through hydrolysis of **2** and subsequent benzyl-esterification (Scheme 1). The degree of benzyl substitution of **3–5** was controlled with feed amounts of BzlBr and DBU (Table 1). The micelles from polymers **1** and **3–5** were obtained by means of a solvent evaporation–sonication technique. The evaporation process resulted in formation of a thin film composed of a mixture of polymer and drug. Subsequent sonication of this film in water provided a drug-encapsulating polymeric micelle solution.

It is worth pointing out that both Am80 and LE540 were very efficiently encapsulated in the PEG-PBLA and PEG-P(Asp $(Bzl)_x$) polymer micelles (Table 2). A high encapsulation yield of ≥75% of the feed was demonstrated on all polymers examined in the wide range of 33 to 100% of the degree of benzyl substitution. Any precipitate was not formed, and furthermore, insoluble aggregates did not interfere with the filtration. When PEG-P(Asp $(Bzl)_x$) polymers

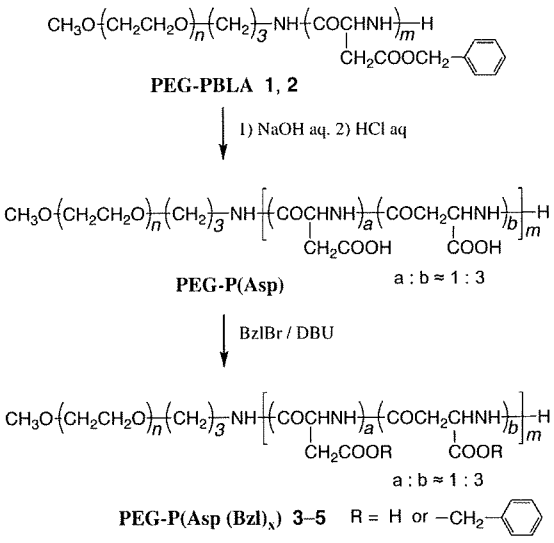

Polymer	n	m	D.s. Bzl* (%)
1	117	24	100
2	117	28	100
3	117	24	80
4	117	24	53
5	117	24	33

* Degree of benzyl substitution.

Scheme 1. Synthetic scheme of PEG-P(Asp (Bzl)$_x$) from PEG-PBLA.

encapsulated a hydrophobic drug, camptothecin, the benzyl substitution degree significantly affected the drug encapsulation efficiency [29]. It was reported that an encapsulation yield of camptothecin reached >90% at 69% of the benzyl substitution degree, however, the yield decreased to <40% at 44% of the substitution. In contrast, Am80 and LE540 were encapsulated at high yields in a wide range of the benzyl ester content of PEG-P(Asp (Bzl)$_x$).

Transparent solutions from polymers **3** and **4** and very faintly hazy ones from polymers **1** and **5** were obtained by means of the evaporation–sonication technique in the presence of a drug. It is important to note that Am80 and LE540 themselves were almost insoluble in water. When the evaporation–sonication technique was applied to the drugs without a polymer, only a slight amount of the drugs (<1% of the feed) was detected in supernatants after the centrifugation. The remaining part of the feed drugs was separated as precipitates. These results indicated that the faintly hazy appearance of the micelle solutions from polymers **1** and **5** was due to particle sizes ≥ca. 140 nm of the polymeric micelles (Table 2), not due to dispersed free drug aggregates.

Interestingly, very low intensity of scattered light was observed in a DLS measurement for a solution of polymer **5** through the evaporation–sonication process without a drug. This result indicated that polymer **5** alone did not form micelle structures as clearly as polymers **1**, **3**, and **4** owing to its low degree (33%) of hydrophobic benzyl substitution. This block copolymer **5** obtained sufficient hydrophobicity to distinctly form micellar structures by physically entrapping the hydrophobic drug. This preferential contribution of the encapsulated drug to the micelle formation can expand choices of block copolymer compositions. Block copolymers possessing hydrophobicity insufficient for the micelle formation can be used for micelle drug-carrier systems if these polymers are successfully given additional hydrophobicity by the encapsulated drugs. This was reported for chemical conjugation of drugs to block copolymers [31], in a doxorubicin-conjugated PEG-P(Asp) system. In contrast, for this Am80 case, the drug was encapsulated in a much easier way, physical entrapment. As far as we know, this is the first report regarding this type of preferential contribution of the physically entrapped drug to polymeric micelles' formation.

Table 2
Encapsulation yield of the drugs and particle size distributions of the polymeric micelles.[a]

Polymer	Am80 encapsulation		LE540 encapulation		Empty
	% Drug encapsulated	Particle size (nm); weight fraction	% Drug encapsulated	Particle size (nm); weight fraction	Particle size (nm); weight fraction
1	94	42±9; 81% 151±29; 19%	82	52±10; 71% 148±28; 29%	60±28; 100%
3	105	21±4; 100%	109	17±3;92% 73±13;8%	7±1; 85% 21±4; 15%
4	101	20±4; 100%	100	23±5; 100%	17±3;100%
5	75	188±37;94% 817±91;6%	94	54±8; 66% 137±24; 34%	–[b]

[a] Weight distributions.
[b] Very low intensity of scattered light.

3.2. Drug release from micelles in vitro

In vitro drug-release rates were measured by means of a dialysis method. The sealed dialysis bag containing the drug-encapsulating micelle solution was placed in a container of D-PBS or water. Using HPLC, we monitored the drug's release from the micelles into an aqueous medium outside the dialysis bag. The experiments were carried out by the use of the micelle solutions summarized in Table 2. These micelle solutions contained Am80 and LE540 in the concentration range of 0.37–0.53 mg/mL and 0.41–0.54 mg/mL, respectively.

A rapid release of Am80 occurred in D-PBS. Approximately 60% of the encapsulated Am80 was released within 8 h for all polymers as shown in Fig. 1. We observed no influence of the polymers' benzyl substitution degree on the release rate. Am80 was soluble in D-PBS at ≥200 μg/mL at r.t. as opposed to Am80's poor solubility of 2 μg/mL in water under the same conditions. Such high solubility in D-PBS is likely to accelerate the rapid release. The observed release rates in this evaluation seem to be too fast for drug targeting purposes, since a blood-circulation period of 24 h or more was necessary for the EPR effect's efficient passive targeting to a solid tumor tissue [2]. The rapid drug-release behaviors shown in Fig. 1 suggest a situation where most of the encapsulated drug is released in the blood stream before the drug carrier system accumulates at the tumor tissue.

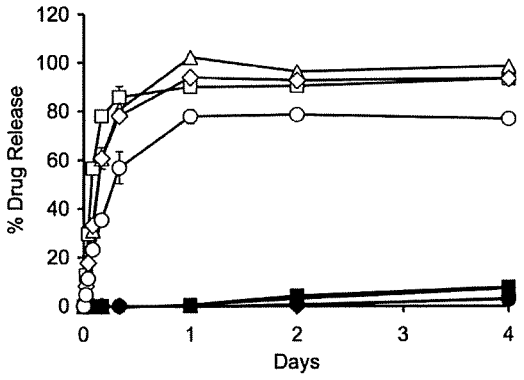

Fig. 1. Release of Am80 and LE540 from the polymeric micelles at r.t. in D-PBS (mean ± SD, $n = 3$). The drug-encapsulating micelles were prepared from polymer **1** (circle), **3** (diamond), **4** (triangle), and **5** (square). Open and filled symbols indicate Am80 and LE540, respectively. The amounts of drug encapsulated in polymeric micelles were normalized to 100%.

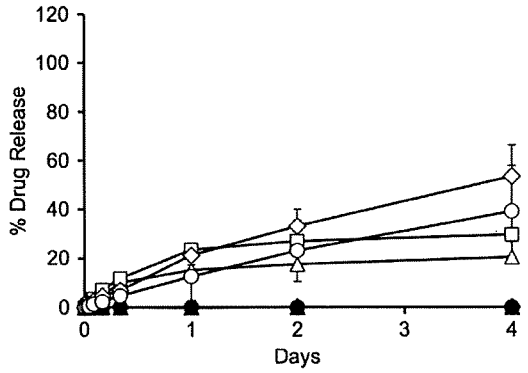

Fig. 2. Release of Am80 and LE540 from the polymer micelles at r.t. in water (mean ± SD, $n = 3$). The drug-encapsulating micelles were prepared from polymer **1** (circle), **3** (diamond), **4** (triangle), and **5** (square). Open and filled symbols indicate Am80 and LE540, respectively. The amounts of drug encapsulated in polymeric micelles were normalized to 100%.

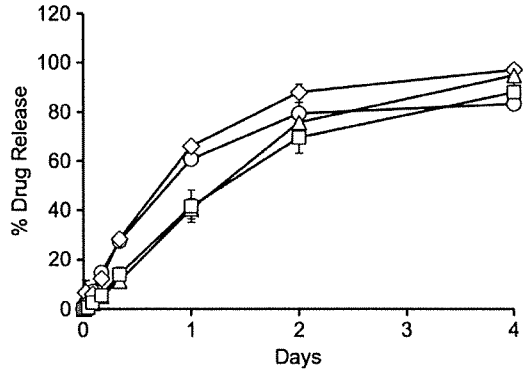

Fig. 3. Release of Am80 from the polymeric micelles at r.t. in D-PBS (mean ± SD, $n = 3$). The Am80-encapsulating micelles were prepared from polymer **1** (circle), **3** (diamond), **4** (triangle), and **5** (square) in the presence of DMDA at various molar ratios to Am80 (circle = 1, diamond = 2.7, triangle = 5.4, and square = 7.5). The amounts of drug encapsulated in polymeric micelles were normalized to 100%.

As compared with the release in D-PBS, considerable release retardation of Am80 was observed in water as shown in Fig. 2. Accumulated Am80 release amounts after 8 h were only 5–12%. Even 4 days later, the released Am80 amounts remained in a range of 20–53%. These results demonstrated that the release rates of Am80 in D-PBS as a dialysate were dramatically differed from the release rates to Am80 in water as a dialysate. This difference was probably due to a difference in Am80 solubility in these solvents. In the release experiments in water, small amounts of powdery precipitates appeared in the dialysis bag within 1–2 days except for the micelles of polymer **1**. This precipitate seems to have been the released Am80. The poor solubility of Am80 in water is likely to lead to saturation in the dialysis bag prior to Am80'a diffusion into the exterior. All these results imply that the poor Am80 solubility in water favors very high encapsulation efficiency, and that the higher solubility in D-PBS than in water causes a rapid release of Am80 from micelles.

In contrast, LE540 was scarcely released either in D-PBS or in water throughout the time period examined, indicating LE540's very stable encapsulation of the synthetic retinoid into the polymeric micelles, as shown in Figs. 1 and 2. Only 3–8% of release was observed in D-PBS over the course of 4 days. This stable encapsulation probably resulted from stronger hydrophobicity of LE540 than of Am80.

3.3. Addition of *N,N*-dimethyldodecylamine (DMDA)

To accomplish more stable encapsulation of Am80, we investigated complex formation of Am80 with a hydrophobic additive. A hydrophobic fatty amine was selected for this purpose. First, *N,N*-dimethyldodecylamine (DMDA) was mixed with Am80 and the polymer in THF, and the mixture was applied to the evaporation–sonication process for the encapsulation. The molar ratio of DMDA to Am80 (DMDA/Am80) was adjusted to 1.0, 2.7, 5.4, and 7.5 for the micelles of polymers **1**, **3**, **4**, and **5**, respectively. These amounts of DMDA corresponded to the molar equivalent of all carboxyl groups of Am80 and aspartic acid residue of a polymer. High Am80 encapsulation yields >94% were confirmed (Table 3; Entries 1, 5, 7, and 9), indicating that the presence of DMDA did not lower the drug encapsulation efficiency. The particle sizes of the polymeric micelles prepared with DMDA did not show a substantial change compared with those prepared without this additive (Table 3; Entries 1, 5, and 7). The only exception was the case of polymer **5**, where the particle diameter decreased from ca. 200 nm to <10 nm upon the addition of DMDA (Table 3; Entry 9). This unique result was found only for polymer **5**, which exhibited distinctive micelle formation only after encapsulation of Am80. (As described above, only polymer **5** did not form a micelle structure.) Although the mechanism for this behavior has not been elucidated, this exceptional result was not observed for the other polymers that formed micelle structures even in the absence of the encapsulated drug.

A remarkable effect of the DMDA addition was a significant retardation in Am80 release from the polymeric micelles in D-PBS, as shown in Fig. 3. A period of 2 days was necessary to attain 60% release of the encapsulated Am80, while the same amounts were rapidly released within 8 h in the absence of DMDA (Fig. 1). At 8 h of the release period, the retardation of Am80 release by means of the DMDA addition indicated statistically significant differences ($P<0.05$) in each polymeric micelle as compared with each micelle without the DMDA addition.

Two mechanisms should be considered to explain these results. The first is a hydrophobic complex formation of Am80 between DMDA. A hydrophilic carboxylic group of Am80 is assumed to greatly

Table 3
Encapsulation of Am80 into the polymeric micelles in the presence of DMDA.

Entry	Polymer	DMDA/Am80[a]	% AM80 encapsulated	Particle size (nm); weight fraction
1	**1**	1	94	36±4; 56%, 135±26; 24%, 639±110; 20%
2	**1**	2.7	97	43±8; 77%, 135±25; 17%
3	**1**	5.4	103	66±24; 89%, 679±109; 11%
4	**1**	7.5	101	54±14; 77%, 817±102; 23%
5	**3**	2.7	97	14±0; 64%, 32±7; 35%, 817±102; 1%
6	**4**	1	100	24±7; 100%
7	**4**	5.4	101	13±2; 97%, 39±8; 3%
8	**4**	10.7	90	22±4; 100%
9	**9**	7.5	104	4±0; 74%, 8±1; 26%

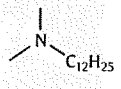

N,N-dimethyl-dodecylamine (DMDA)

[a] Molar ratio.

contribute to the high solubility of Am80 in D-PBS. Therefore, conversion of this group to a more hydrophobic state is probably effective in decreasing the solubility. An ionic compound's solubility can be changed by means of an electrostatic interaction between an opposite charged hydrophobic compound, and researchers have used the effect as the "hydrophobic ion-pairing" technique [32,33]. This technique serves to increase the hydrophobicity of hydrophilic ionic compounds including a drug [33,34] as well as a protein and polynucleotide [32]. For example, a potent antituberculosis drug, isonicotinic acid hydrazide, was chemically converted into an ionic compound as a prodrug, and the hydrophobic ion-pairing significantly enhanced drug's solubility to an organic solvent [33]. Furthermore, skin accumulation of retinoic acid was enhanced by an ion-pairing with a series of hydrophobic amino acid methyl esters [34]. In our study, DMDA is regarded as a hydrophobic counter partner for Am80. This is the first report that the ion-pairing technique has been used for stable drug encapsulation in the polymeric micelle carrier system.

The second mechanism that explains the effect of DMDA is a change of micellar core characteristics by encapsulation of a hydrophobic additive. Forrest et al. reported that encapsulation of α-tocopherol (vitamin E) into PEG-b-poly(ε-caprolactone) (PEG-PCL) micelles decreased the viscosity of the crystalline PCL core owing to dispersed microphases of α-tocopherol [23]. Such a plasticized PCL core was receptive to a larger amount of rapamycin loading. Furthermore, the α-tocopherol-co-encapsulating micelle demonstrated a retardation of the drug release in PBS containing bovine serum albumin as compared with the PEG-PCL micelle formed without α-tocopherol.

If DMDA contributes to the sustained release of Am80 mainly by means of the hydrophobic ion-pairing, this contribution increases up to the DMDA addition at the DMDA/Am80 molar ratio of 1. On the other hand, if DMDA acts to change the characteristics of the micellar core, the retardation effect by DMDA relies on the amount of added DMDA beyond the DMDA/Am80 ratio of 1. Therefore, we investigated the effects of an added DMDA amount by using polymers **1** and **4**. When DMDA was added to a mixture of polymer **1** and Am80 in the range of the DMDA/Am80 ratio from 1.0 to 7.5 (Table 3; Entries 1–4), the drug-release rate underwent no significant changes, as shown in Fig. 4. This result indicated that the retardation of the Am80 release was due to the hydrophobic ion-pairing of Am80 and DMDA for the polymer **1** case. On the other hand, the retardation of the drug release was observed at the DMDA/Am80 ratio ≥ 5.4 for the micelle of polymer **4** as shown in Fig. 5. The retardation effect hardly exhibited itself at the

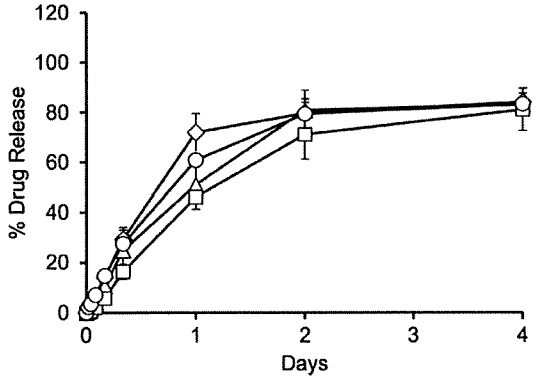

Fig. 4. Release of Am80 from the micelles of polymer **1** at r.t. in D-PBS (mean ± SD, $n = 3$). The Am80-encapsulating micelles were prepared in the presence of DMDA at various molar ratios to Am80 (circle = 1, diamond = 2.7, triangle = 5.4, and square = 7.5). The result at the ratio of 1 represented in Fig. 3 was shown again for the comparison with the results at the other ratios. The amounts of drug encapsulated in polymeric micelles were normalized to 100%.

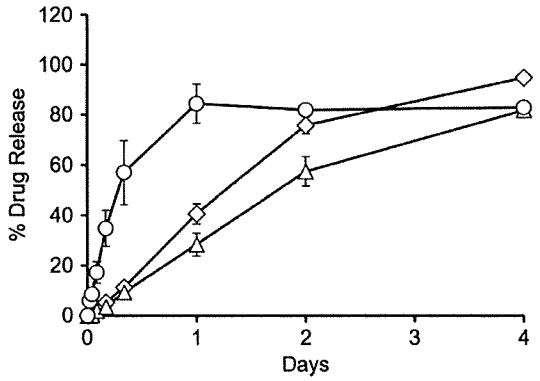

Fig. 5. Release of Am80 from the micelles of polymer **4** at r.t. in D-PBS (mean ± SD, $n = 3$). The Am80-encapsulating micelles were prepared in the presence of DMDA at various molar ratios to Am80 (circle = 1, diamond = 5.4, and triangle = 10.7). The result at the ratio of 5.4 represented in Fig. 3 was shown again for the comparison with the results at the other ratios. The amounts of drug encapsulated in polymeric micelles were normalized to 100%.

DMDA/Am80 ratio of 1. This deficient retardation was probably due to the presence of the carboxyl group of polymer **4**. This carboxyl group would compete with the carboxyl group of Am80 for interaction with DMDA. Therefore the excess amount of DMDA going to Am80 was necessary for the obvious retardation. In fact, the molar amount of DMDA at a DMDA/Am80 molar ratio of 5.4 in which the substantial retardation effect was demonstrated was equal to the molar amount of all the carboxyl groups of Am80 and polymer **4**. Two mechanisms serve to explain the observed retardation, as shown in Fig. 5. The first is an increase in the hydrophobicity of Am80 caused by the ion-pairing with DMDA as described above. The second is a change of characteristics of the micelle inner core accompanying the pairing of the carboxyl group of polymer **4** and DMDA. It is difficult to indicate which mechanism dominantly contributed to the retardation, since the current study did not separate the effect on Am80 from that on the polymer.

Zeta potential of empty polymeric micelles except for the micelles of polymer **5** was -5.6 ± 0.2 to -12.6 ± 1.3 mV; see Supplementary Table S1. These values were slightly decreased with the Am80 encapsulation (-9.9 ± 0.0 to -22.1 ± 0.7 mV). Although the DMDA addition raised the zeta potential, the micelles kept negative surface charges under the conditions for the retardation experiments of the Am80 release.

As described above, the addition of DMDA successfully triggered the retardation of the Am80 release. The presumption is that the triggering mechanism involved the hydrophobic complex formation between Am80 and DMDA, and the encapsulation of this complex in the polymeric micelle. Therefore, we investigated not only Am80 but also the co-encapsulation of DMDA into the polymeric micelle.

The polymeric micelle solutions prepared in the presence of Am80 and DMDA were ultrafiltered with a Microcon YM-100 (100-kDa cut-off). This process separated the polymeric micelles in the retentate from low-molecular compositions in the filtrate. A retentate is a residual solution on an ultrafilter membrane after the ultrafiltration, and a filtrate is a solution that has passed through the ultrafilter. The amounts of Am80 and DMDA both in the retentate and the filtrate were measured by means of an HPLC. Six samples were applied to this separation experiment, as summarized in Table 4. The sample solutions included DMDA, polymer **1**, and Am80 (Entry 1), DMDA alone (Entries 2 and 3), DMDA and polymer **1** (Entry 4), and DMDA and Am80 (Entries 5 and 6). We prepared the solutions by using the evaporation–sonication process.

Approximately 76% of the feed DMDA was recovered in the sample solutions prepared in the presence of polymer **1** and Am80 (Table 4;

Table 4
Compositions of sample solutions for the separation experiments and percent recovery of DMDA and Am80.

Entry	Feed				% Recovered					
	DMDA mg (μmol)	Polymer 1 mg	Am80 mg (μmol)	DMDA/ Am80[a]	DMDA			Am80		
					Sample solution	Retentate[b]	Filtrate[b]	Sample solution	Retentate*	Filtrate **
1	1.2 (5.69)	20.0	2.0 (5.69)	1	75.8	50.7 ± 1.5	9.7 ± 1.2	83.9	63.2 ± 0.4	0.2 ± 0.0
2	1.2 (5.69)	–	–	–	0	–	–	–	–	–
3	6.5 (30.5)	–	–	–	10.7	0	8.7 ± 0.5	–	–	–
4	1.2 (5.69)	20.0	–	–	28.6	4.5 ± 0.4	13.3 ± 1.7	–	–	–
5	1.2 (5.69)	–	2.0 (5.69)	1	0	–	–	0.4	–	–
6	6.5 (30.5)	–	2.0 (5.69)	5.4	17.7	N.D.[c]	13.5 ± 0.5	100.1	N.D.***	35 ± 0.7

[a] Molar ratio.
[b] Mean ± SD ($n = 3$).
[c] N.D. means not determined.

Entry 1). This recovered DMDA remained in the retentate (50.7% of the feed) even after the ultrafiltration (Table 4; Entry 1). Simultaneously, we observed that Am80 in this sample solution was 83.9% of the feed. Moreover, after the ultrafiltration, 63.2% of the feed remained in the retentate, and only 0.2% of the feed was found in the filtrate. In contrast, in the examination for DMDA alone, we observed that a serious loss of feed DMDA (only recovered <11% of the feed) probably caused by adsorption of DMDA to a 0.22 μm filter in the sample preparation process (Table 4; Entries 2 and 3). Moreover, almost all of the recovered DMDA was ultrafiltered into the filtrate, and no DMDA was found in the retentate (Table 4; Entry 3). Remaining DMDA (ca. 20%) was probably adsorbed to a Microcon YM-100 filter. These results support the assertion that both Am80 and DMDA were encapsulated into polymeric micelles. Although the encapsulation of DMDA into polymeric micelles was also observed in the absence of Am80 (Table 4; Entry 4), DMDA in the sample solution was only <30% of the feed (Table 4; Run 4). In addition, a half of the recovered DMDA was ultrafiltered into the filtrate. Therefore, the stable encapsulation of DMDA in the micelles of polymer **1** was achieved by means of the co-encapsulation of DMDA with Am80.

When DMDA was mixed with Am80 at an equal molar ratio (DMDA/Am80 = 1), an insoluble aggregate was formed during sonication. After removal of the aggregate by means of centrifugation, no DMDA and only 2 μg/mL of Am80 (<1% of the feed) remained in the supernatant (Table 4; Entry 5). Under the same conditions in the presence of polymer **1**, such an insoluble aggregate was not observed, and a high encapsulation yield of Am80 (84%) was obtained (Table 4; Entry 1). These contrast results indicate two points: first, the complex of Am80 and DMDA that formed at DMDA/Am80 of 1 was insoluble in water, and second, the solubilization of the complex depended on encapsulation of the complex into the polymeric micelles. In contrast to the results at DMDA/Am80 = 1, the mixture at DMDA/Am80 = 5.4 provided a transparent solution by means of sonication. This solution contained 17.7% and 100% of the feed for DMDA and Am80, respectively, indicating that DMDA both formed a low-molecular micelle and encapsulated Am80 (Table 4; Entry 6). This Am80-DMDA solution, however, formed an insoluble aggregate in the retentate during the ultrafiltration procedure. Almost all of the recovered DMDA was ultrafiltered into the filtrate. In contrast, only 3.5% of the feed Am80 was found in the filtrate. This result implied that the Am80-encapsulating DMDA micelles were dissociated in the ultrafiltration and that the Am80 was no longer encapsulated in the DMDA micelles. In addition, this result also indicated that the retardation of the Am80 release was not caused by a sustained release from the Am80-encapsulating DMDA micelle. If Am80 had been dominantly encapsulated in the DMDA micelle but not the polymeric micelle, the aggregate would have been observed in the ultrafiltration of the experiment for Entry 1. In fact, no such aggregate was observed. Therefore, the retarded release of Am80 was accomplished by the co-encapsulation of the drug and DMDA in the polymeric micelles.

3.4. Effects of an additive's structure on the release of Am80

We investigated the effects that chemical structure of an additive has on the retardation of Am80 release by using six kinds of amines, as shown in Chart 2. We added these amines to the encapsulation process of the Am80. The added amounts of the additives were adjusted to additive/Am80 molar ratio of 1. The micelles were prepared from polymer **1** in order to ignore the influence of the carboxyl groups of the polymer. High Am80 encapsulation yields between of 61% and 96% were obtained in all additives examined as summarized in Table 5.

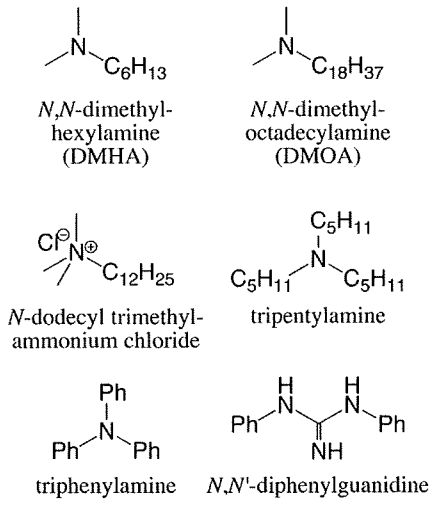

Chart 2. Amines examined for the retardation effect on the Am80 release.

Table 5
Encapsulation of Am80 into the polymeric micelles in the presence of various additives.

Entry	Additive	% Am80 encapsulated	Particle size (nm); weight fraction
1	*N,N*-dimethylhexylamine	96	86 ± 14; 79%, 215 ± 36; 21%
2	*N,N*-dimethyloctadecylamine	80	74 ± 13; 22%, 231 ± 45; 78%
3	*N*-dodecyltrimethylammonium chloride	78	69 ± 13; 71%, 195 ± 37; 29%
4	Tripentylamine	61	65 ± 11; 86%, 185 ± 33; 14%
5	Triphenylamine	88	79 ± 14; 76%, 224 ± 41; 24%
6	*N,N'*-diphenylguanidine	91	34 ± 6; 87%, 138 ± 24; 13%

The Am80 release was measured once for each additive-co-encapsulating micelle, as shown in Fig. 6. Of the six additives, *N,N*-dimethyloctadecylamine (DMOA) demonstrated the largest retardation effect on the Am80 release. The other five additives showed only small effects for the retardation. These results were likely caused either by undesired steric hindrance, inhibiting the interaction between Am80 and the amines, or by an insufficient increase in the hydrophobicity of the Am80-complex. A series of the *N,N*-dimethylalkylamines exhibit a decrease the release rates of Am80 with an increase of the alkyl chain length. This effect was confirmed in separate triplicate examinations as shown in Fig. 7. A comparison of three *N,N*-dimethylalkylamines, i.e., DMOA, DMDA, and *N,N*-dimethylhexylamine (DMHA), clearly showed the effect of the chain length. This result indicates that the counter additive selection can control the release rate of Am80 from a polymeric micelle. At 1 day of the release period, the retardation effects by means of DMOA or DMDA addition were statistically significant (DMOA; $P<0.001$ and DMDA; $P<0.01$) in comparison with the control group (encapsulation of Am80 alone; filled square in Fig. 7). On the other hand, a difference from the control system by means of DMHA addition was statistically insignificant at $P>0.05$.

Cytotoxicities of *N,N*-dimethylalkylamines were evaluated by means of a standard in vitro cytotoxicity test; see Supplementary Fig. S1. The results were compared with that of 1-octadecylamine (stearylamine), frequently used in vivo as a component of liposomal carriers [35]. DMDA and DMOA, two additives that showed sufficient retarded release effect, exhibited a similar cytotoxicity to 1-octadecylamine. These results indicate that toxicity of these additives can be acceptable to use in vivo depending on toxicity of encapsulated drugs. DMHA, hardly effective for retarded release, exhibited no cytotoxicity up to 100 μM. The next challenge is in vivo studies to validate this release rate control by means of the ion-pairing technique.

4. Conclusions

Two synthetic retinoids, Am80 and LE540, were encapsulated into block copolymer micelles, and the encapsulation was both highly efficient and exceptionally facile. An in vitro release examination for LE540 demonstrated very stable encapsulation of this drug. As for Am80, it was rapidly released in D-PBS in contrast to Am80's sustained release in water. We triggered a retardation of the release rate of Am80 by adding DMDA into the encapsulation process. This retardation was due to an increase in the hydrophobicity of Am80, itself caused by the ion-pairing of this retinoid with hydrophobic DMDA. The retardation effect increased with increase in the alkyl chain length of additive amines, suggesting that proper choice of an additive amine leads to optimum control of drug release. This is the first report concerning the ability of ion-pairing between a drug and an additive to promote control a drug's release rate in a polymeric micelle carrier system. This ion-pairing technique requires only the mixing of an adequate additive without any chemical modification of the drug or the polymers. Thus, it appears highly promising that this simple technique is applicable to various drugs possessing an ionic group.

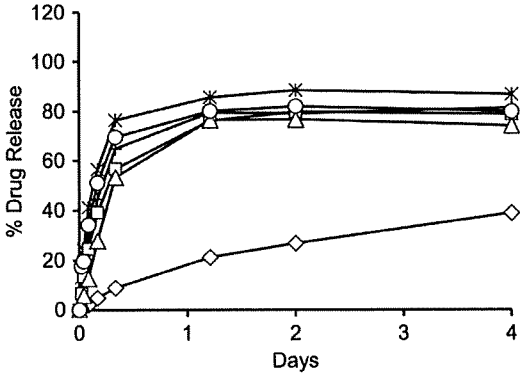

Fig. 6. Release of Am80 from the micelles of polymer **1** at r.t. in D-PBS ($n=1$). The Am80-encapsulating micelles were prepared in the presence of various amine additives at an equal molar ratio to Am80 (circle = *N,N*-dimethylhexylamine, diamond = *N,N*-dimethyloctadecylamine, triangle = *N*-dodecyltrimethylammonium chloride, square = tripentylamine, asterisk = triphenylamine, and cross = *N,N'*-diphenylguanidine). The amounts of drug encapsulated in polymeric micelles were normalized to 100%.

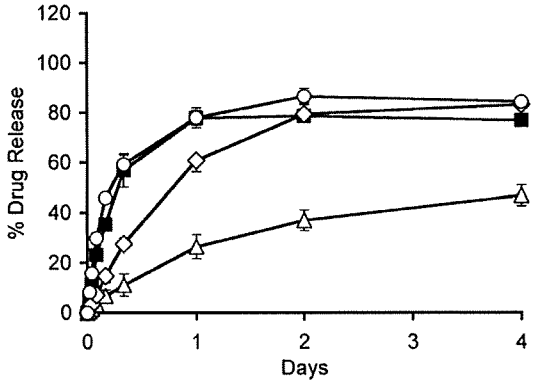

Fig. 7. Release of Am80 from the micelles of polymer **1** at r.t. in D-PBS (mean ± SD, $n=3$). The Am80-encapsulating micelles were prepared in the presence of various *N,N*-dimethylalkylamines at an equal molar ratio to Am80 (circle = *N,N*-dimethylhexylamine, diamond = *N,N*-dimethyldodecylamine, triangle = *N,N*-dimethyloctadecylamine, and filled square = no additive). The results of *N,N*-dimethyldodecylamine represented in Fig. 3 and no additive group represented in Fig. 1 were shown again for the comparison with the results of the other groups. The amounts of drug encapsulated in polymeric micelles were normalized to 100%.

Acknowledgement

This work was supported by the Ministry of Health, Labour, and Welfare of Japan, and JST, CREST, Japan. T. Satoh and M. Yokoyama acknowledge the support from the Program for Promoting the Establishment of Strategic Research Centers, Special Coordination Funds for Promoting Science and Technology, the Ministry of Education, Culture, Sports, Science and Technology of Japan.

Appendix A. Supplementary data

Supplementary data associated with this article can be found, in the online version, at doi:10.1016/j.jconrel.2009.02.024.

References

[1] S.R. Croy, G.S. Kwon, Polymeric micelles for drug delivery, Curr. Pharm. Des. 12 (2006) 4669–4684.
[2] Y. Matsumura, H. Maeda, A new concept for macromolecular therapeutics in cancer chemotherapy: mechanisms of tumoritropic accumulation of protein and the antitumor agent SMANCS, Cancer Res. 46 (1986) 6387–6392.
[3] M. Yokoyama, T. Okano, Y. Sakurai, S. Fukushima, K. Okamoto, K. Kataoka, Selective delivery of adriamycin to a solid tumor using a polymeric micelle carrier system, J. Drug Target. 7 (1999) 171–186.
[4] M.L. Forrest, J.A. Yáñez, C.M. Remsberg, Y. Ohgami, G.S. Kwon, N.M. Davies, Paclitaxel prodrugs with sustained release and high solubility in poly(ethylene glycol)-b-poly(ε-caprolactone) micelle nanocarriers: pharmacokinetic disposition, tolerability, and cytotoxicity, Pharm. Res. 25 (2008) 194–206.
[5] M. Watanabe, K. Kawano, M. Yokoyama, P. Opanasopit, T. Okano, Y. Maitani, Preparation of camptothecin-loaded polymeric micelles and evaluation of their incorporation and circulation stability, Int. J. Pharm. 308 (2006) 183–189.
[6] M. Sumitomo, F. Koizumi, T. Asano, A. Horiguchi, K. Ito, T. Asano, T. Kakizoe, M. Hayakawa, Y. Matsumura, Novel SN-38-incorporated polymeric micelle, NK012, strongly suppresses renal cancer progression, Cancer Res. 68 (2008) 1631–1635.
[7] S. Kawakami, P. Opanasopit, M. Yokoyama, N. Chansri, T. Yamamoto, T. Okano, F. Yamashita, M. Hashida, Biodistribution characteristics of all-trans retinoic acid incorporated in liposomes and polymeric micelles following intravenous administration, J. Pharm. Sci. 94 (2005) 2606–2615.